NTIA Report 87-221

Wideband HF Modeling and Simulation

J. A. Hoffmeyer
M. Nesenbergs

U.S. DEPARTMENT OF COMMERCE
Malcolm Baldrige, Secretary

Alfred C. Sikes, Assistant Secretary
for Communications and Information

July 1987

PREFACE

Certain commercial equipment, instruments, or materials are identified in this paper to specify adequately the experimental procedure. In no case does such identification imply recommendation or endorsement by the National Telecommunications and Information Administration, nor does it imply that the material or equipment identified is necessary the best available for the purpose.

CONTENTS

LIST OF FIGURES

LIST OF FIGURES (continued)

LIST OF TABLES

LIST OF ACRONYMS

A/D	analog to digital
AI	artificial intelligence
AJ	antijamming
AWGN	additive white Gaussian noise
bps	bits per second
BW	bandwidth
CCIR	International Radio Consultive Committee
CF	critical frequency
cw	continuous wave
DAC	delay adaptive combiner
DFE	decision feedback equalizer
DS	direct sequence
EM	electromagnetic (waves)
EW	electronic warfare
FACS	Frequency Agile Communication System
FH	frequency hopping
FOT	Frequency of Optimum Transmission
FPIS	forward propagation by ionospheric scatter
HF	high frequency
IF	intermediate frequency
IFS	ionospheric forward scatter
IONCAP	Ionospheric Communications Analysis and Prediction Program
ITS	Institute for Telecommunication Sciences
JF	junction frequency
kHz	kilohertz
LF	low frequency
LFM	linear frequency modulation
LOF	lowest operating frequency
LPI	low probability of interception
LUF	lowest usable frequency
MHz	megahertz
MUF	maximum usable frequency

LIST OF ACRONYMS (continued)

NB	narrowband
NOSC	Naval Ocean Systems Center
NRL	Naval Research Laboratory
NTIA	National Telecommunications and Information Administration
O	ordinary (ray)
PLL	phase-lock loop
PN	pseudonoise
PSK	phase-shift keying
rf	radio frequency
RFI	radio frequency interference
rms	root-mean square
RSL	received signal level
SID	sudden ionospheric disturbance
SNR	signal-to-noise ratio
SS	spread spectrum
SSN	Sunspot Number
TDL	tapped delay line
VLF	very low frequency
WB	wideband
X	extraordinary (ray)

WIDEBAND HF MODELING AND SIMULATION

J. A. Hoffmeyer and M. Nesenbergs*

Laboratory testing of proposed and new wideband (e.g., spread spectrum) high frequency (HF) systems is currently not possible because wideband HF channel simulators do not exist. Moreover, there are no validated HF channel models for bandwidth on the order of a megahertz on which to base simulator designs with confidence. Enhanced measurement programs over appropriate radio paths are needed to verify the main features of wideband channel models or to propose improvements in the existing narrowband models.

This report starts with an elementary review of ionospheric propagation. It summarizes the recent work in spread spectrum technology targeted for the HF radio band. Thereafter follows a short section devoted to additive distortions, namely noise and interference, also in the HF band. The report next presents an assessment of past narrowband HF models: their background, old validation tests, and--to be quite specific--the NTIA/ITS development of the Watterson simulator. That laboratory tool, judged best by many, works in real time and offers accurate representations of HF channel bandwidth up to 10 or 12 kHz.

In the present study, an extension to wideband models is attempted. Unfortunately, it suffers from an apparently serious shortage of measured data for the time-varying channel transfer function. A possible wideband model is hypothesized, conjectures are made, and questions are raised. One is left faced with a requirement for an experimental program to ascertain the wideband (1 MHz or more) characteristics of multipath fading for digital radio transmissions in the (2- to 30-MHz) band and over radio propagation paths of interest. Real data on the characteristics of the time-varying channel transfer function would be invaluable for the ongoing simulator work at several research organizations.

Key words: channel simulation; HF channel models; HF propagation; spread spectrum; wideband communications

1. INTRODUCTION

The Institute for Telecommunication Sciences, National Telecommunication and Information Administration is conducting a project to determine the feasibility of wideband high frequency (HF) channel simulation. The five tasks of this project, sponsored by the Joint Tactical Command Control and Communications Agency Test Element, are

---

*The authors are with the Institute for Telecommunication Sciences, National Telecommunications and Information Administration, U.S. Department of Commerce, Boulder, CO 80303-3328.

- Task 1 - Study general characteristics of spread spectrum HF radios
- Task 2 - Study the characteristics of available HF channel simulators
- Task 3 - Investigate wideband HF propagation models
- Task 4 - Define requirements for a wideband HF channel simulator
- Task 5 - Develop a functional block diagram for a wideband HF channel simulator.

The ultimate objective, which is beyond the scope of the present project, is to develop a wideband simulator to be used in the real-time performance evaluation of spread spectrum HF radios.

Several questions follow immediately from this stated objective. The first is: What are the characteristics of the class of spread spectrum radios to be tested? The objective is not to simulate the HF radio but rather to simulate the HF channel. This requires general knowledge of spread spectrum radio signal parameters, such as instantaneous bandwidth and frequency hopping characteristics, but not detailed knowledge of other aspects of the radio, such as transmitter/receiver implementation and hardware. The bandwidth of the radios to be tested will dictate the bandwidth requirements of the HF channel simulator.

Additional questions are; What channel simulators are currently available, and what are their general characteristics? Do they have the capability for testing spread spectrum radios that are currently available or are in the design and development stage? If the answer to this latter question is negative, then further research and development programs may be needed for the development of new HF channel simulators.

Tasks 1 and 2 of this project address these questions. The answers are not easy because of uncertainty in the communications community as to the capacity of the HF channel to support extremely wide (of the order of 1 to 5 MHz) sky-wave radio channels. The complexity and time variability of the HF channel have been addressed by many researchers. The assessment of the performance of a wideband radio in this dynamically changing environment is directly related to the requirements of the system user. Thus for some applications, wideband HF appears feasible, while for other applications the feasibility is less certain.

Figure 1 depicts the interrelationship of wideband measurements, wideband channel models, the medium imposed constraints, and the development of wideband radios and channel simulators. As with all new system development, the evolution starts with requirements as stated by the system user. For spread spectrum systems, these include the need for antijam capability, covert transmission (i.e., low probability of intercept), selective addressing and multiple access, and interference rejection. Interoperability standards are an important requirement especially for military tactical communications. The degree to which these requirements can be fulfilled depends equally upon the state of the art of electronics technology and upon the capacity of the HF channel to support wideband transmissions. The importance of wideband channel measurements cannot be overemphasized. Such measurements are necessary for the development of a channel model to be used as the basis of channel simulators. The measured constraints are also critical inputs for the design and development of wideband radios. As can be seen from Figure 1, the desired overall goal is the real-time performance evaluation of spread spectrum HF radios in the laboratory.

The approach taken in the first two tasks of the study, and as described in this report, has been to conduct an extensive literature search and to contact key people who are working in the field of HF spread spectrum. The automated literature search concentrated on spread spectrum HF and channel simulation. This resulted in the compilation of an extensive bibliography. Many of these documents are referred to in this report and are listed in Section 9.

The emphasis in this report is on the sky-wave propagation of wideband HF signals. The most complex questions are related to sky-wave propagation rather than surface wave.

2. BACKGROUND

2.1 General History

At the start of this century, Marchese Guglielmo Marconi demonstrated trans-Atlantic radio transmissions through what was later to be known as ionospheric propagation. It was about a quarter of a century thereafter when Appleton and others actually demonstrated the existence of ionized layers. The region in question became known as the ionosphere (NBS, 1948; Davies, 1965).

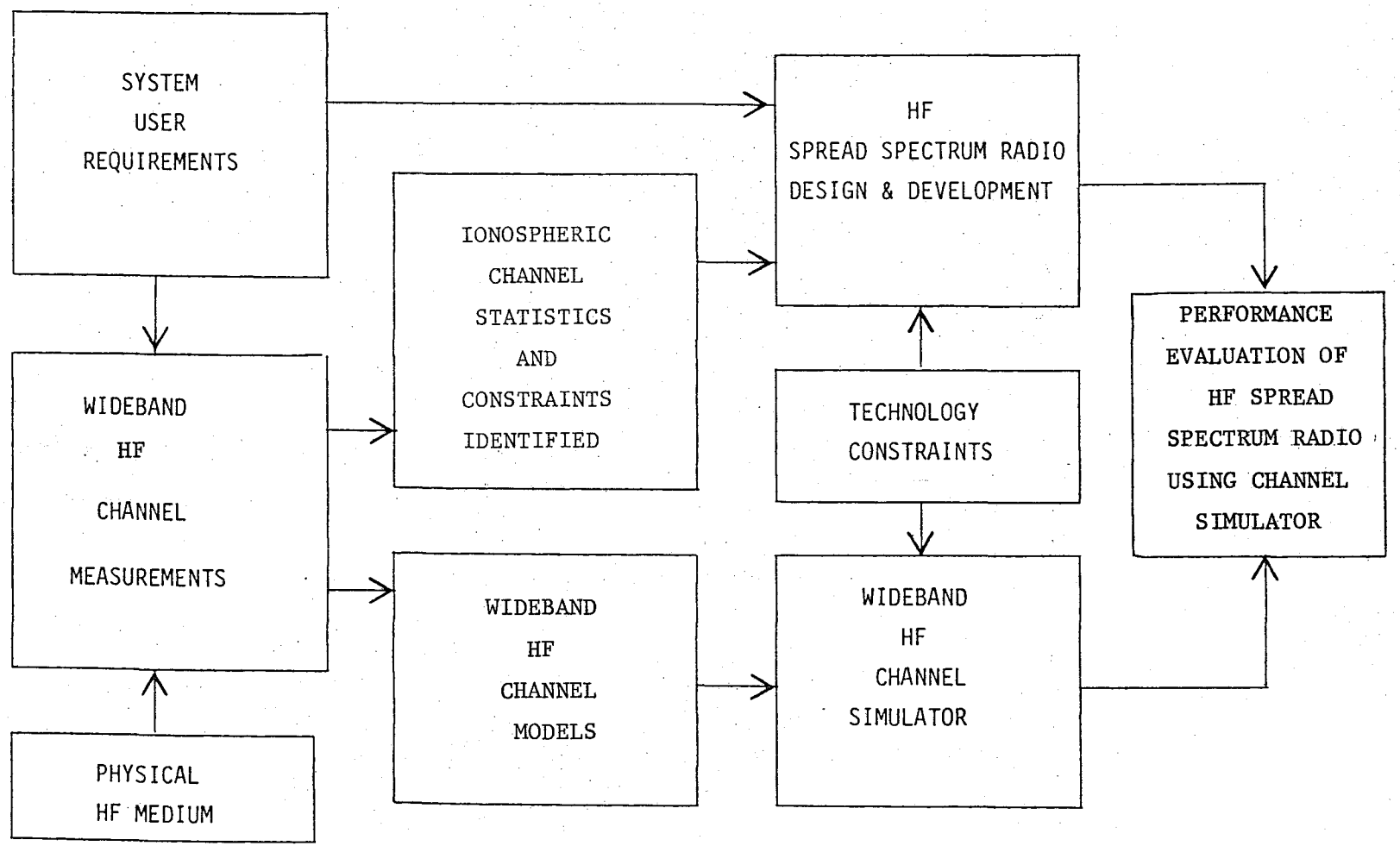

Figure 1. Interrelationship of wideband channel measurements, models, and simulators and the performance evaluation of spread spectrum radios.

It occupies the outermost reaches of the Earth's upper atmosphere, between 100 and 1000 km altitude, where solar radiation creates ionized particles. Certain frequencies, namely those between roughly 2 (or 3) and 30 MHz, can be variously refracted, reflected, and propagated long distances by the layers. As is well known to all telecommunications engineers, this frequency band is called the high frequency (HF) band. The HF band became a useful and inexpensive radio telecommunications tool for assorted analog and digital services (Goldberg, 1966; Folkestad, 1968; CCIR, 1982b). In this respect it remains an important worldwide medium even today (Bowhill, 1981 and 1984; Jull, 1984).

Another quarter of a century passed after Appleton's work before the emergence of modern digital communications. To be effective over HF, digital systems generated a need for HF channel characterization. The early work by Kailath (1961), Price and Green (1958), and others in the fifties and sixties caused a great interest among communication theorists (Bello, 1963; Daly, 1964; Sifford et al., 1965; Shaver et al., 1967; Kennedy, 1969). There followed over the next decade or so a virtual deluge of quantitative, statistical, theoretical, and--to some extent--experimental studies. In response to observed time variations (i.e., distortions) in received signal amplitude, phase, and spectral components--known among communicators as multipath or selective fading--various descriptive channel models evolved.

A simple model of current relevance is the time-varying linear channel. It is graphically introduced in Figure 2. For the purposes of this study, it is assumed that the basic model of a linear time-varying filter plus additive noises or interference remains valid for the HF radio signal path between antennas, regardless the time-and-frequency characteristics of the signal.

In Figure 2, x(t) is the input signal, n(t) is the total additive distortion (e.g., noise and interference), and y(t) is the output signal. All three of these can have various more or less equivalent representations. They can be continuous or discrete, complex or real, at radio frequency (rf), at an intermediate frequency (IF), or at baseband. The fading of the time-varying HF medium is determined by the two-dimensional random function H(f,t). In electronic circuit applications, one may be familiar with the fixed filter and its invariant frequency response, H(f). For the HF channel to be represented by a filter, one must permit the filter to possess the observed, unpredictable,

or random variation in time. One incorporates this phenomenon into H(f,t) via the second argument "t."

Admittedly, many functions have been used to characterize the multiplicative dependence of y(t) on x(t). However, only two are to be employed here. The first is the aforementioned H(f,t). The second is the causal time-varying impulse response, $h(\tau,t)$. It represents the channel response at time t due to an impulse at time $t-\tau$. The two functions are related by a Fourier transform over τ or its conjugate variable. As a consequence, both H(f,t) and $h(\tau,t)$ possess many physical interpretations and offer alternative bases for HF channel modeling. These options will be addressed in more depth in Sections 5 and 6 of this study.

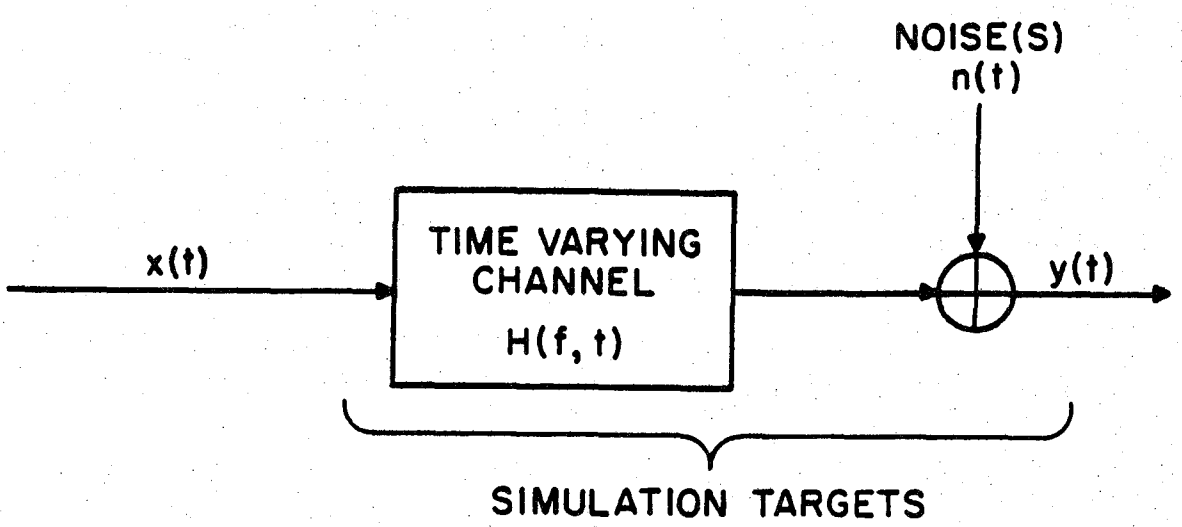

Figure 2. The linear time-varying channel model.

2.2 HF Propagation Characteristics

At this point, it may be convenient to mention briefly the physical multimode or multipath aspects of HF propagation. At a given radio frequency, wave reflection can take place at several regions or layers in the ionosphere. These are called the D, E, F, F1, F2, and other, regions. Figure 3 shows that they correspond in the electron density versus altitude profile to layers of constant density. Of course, the profile in Figure 3 is a hypothetical example. Actual profiles vary in intensity, in time, in space, and are affected by unpredictable solar and geophysical events. Certain layers may or may not be visible to all frequencies, at all times, or at all antenna-beam elevations of interest. Moreover, multihop propagation may occur over longer distances. The HF wave may be reflected from F1, return to the Earth's surface, only to be reflected upward. On its second trip, the wave may reach F1 again, be reflected for a second time, and finally arrive at the receiving antenna. Such a mode would be denoted as 2F1. Of course, there are other possibilities observed more or less frequently. Thus, the number and character of returned modes is almost random. For HF paths in moderate zones, the number of modes can range from zero to a half-dozen.

In the physical world, certain HF sky-wave paths are more typical than others. Several such simple cases are illustrated in Figure 4. Figure 4a depicts radio waves "reflecting" off the E and F layers. The actual mechanism is refraction rather than reflection and a variable number of weaker physical layers may be involved (NBS, 1948; Davies, 1965). The high ray and low ray paths are defined in the figure. Figure 4b depicts multiple hop paths from the transmitter to the receiver, but subject to a single F layer.

2.3 Ionograms

A convenient graphical tool to study the HF channel features is the ionogram. Figure 5 presents two hypothetical ionograms (due to Watterson, 1979). In both Figures 5a and 5b, two major propagation modes are depicted: a single-hop, F-layer mode (designated 1F) and a double-hop, F-layer mode (designated 2F). The hypothetical ionograms correspond to the multiple-hop paths depicted in Figure 4b. The ionograms also contain high and low rays, which correspond to the high and low rays in Figure 4a. Two magnetoionic components, designated ordinary and extraordinary, are also depicted in the

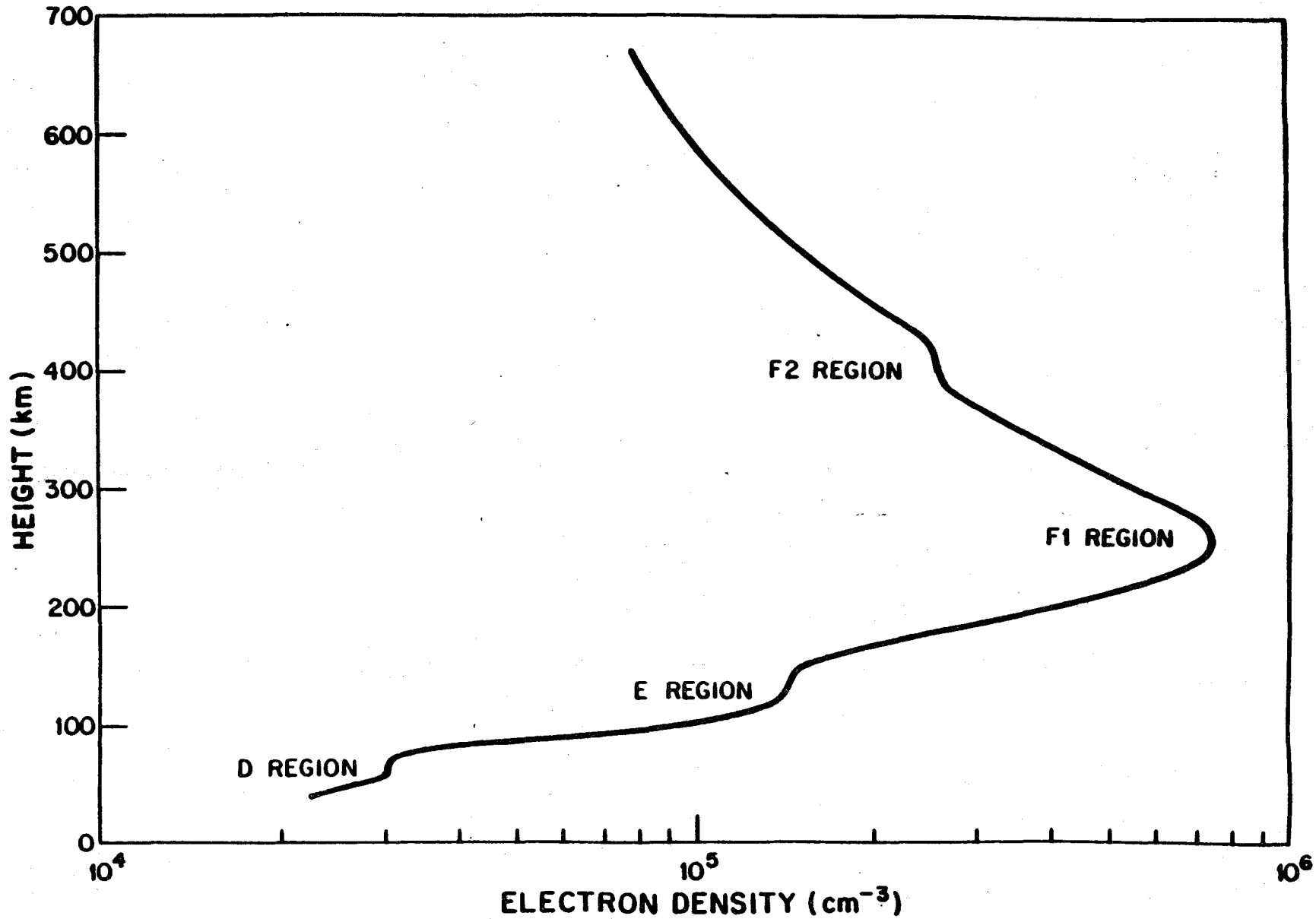

Figure 3. Electron density profile and ionospheric reflection regions.

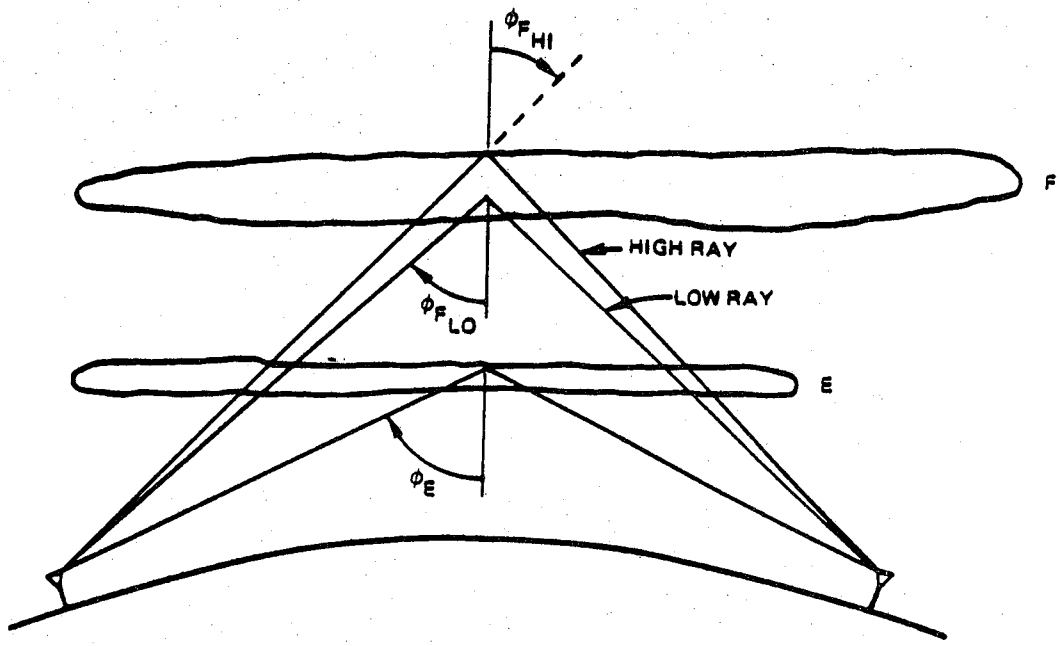

a. Radio waves obliquely reflecting off the E and F layers.

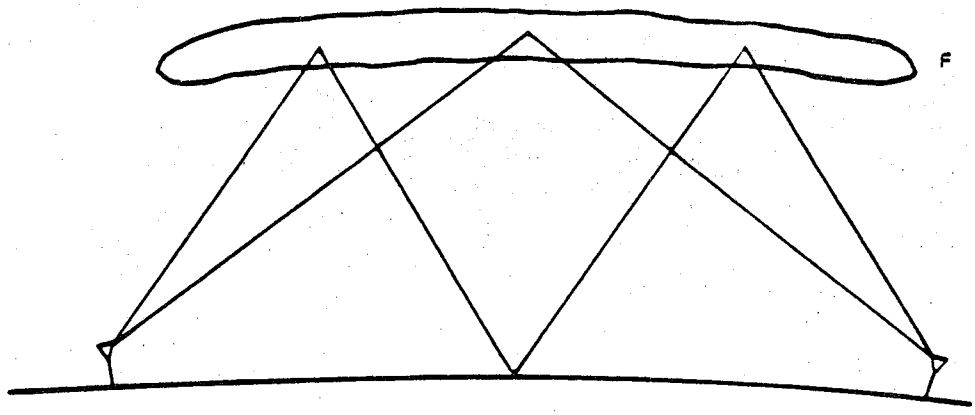

b. Multiple-hop paths from transmitter to receiver.

Figure 4. Examples of HF sky-wave transmission.

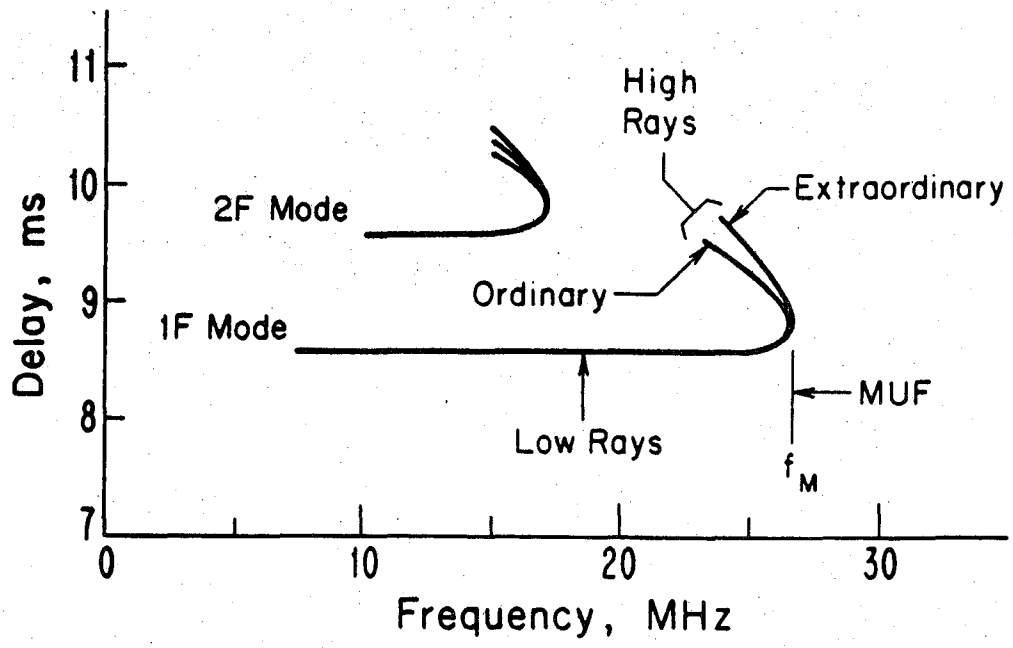

(a) QUIET IONOSPHERE

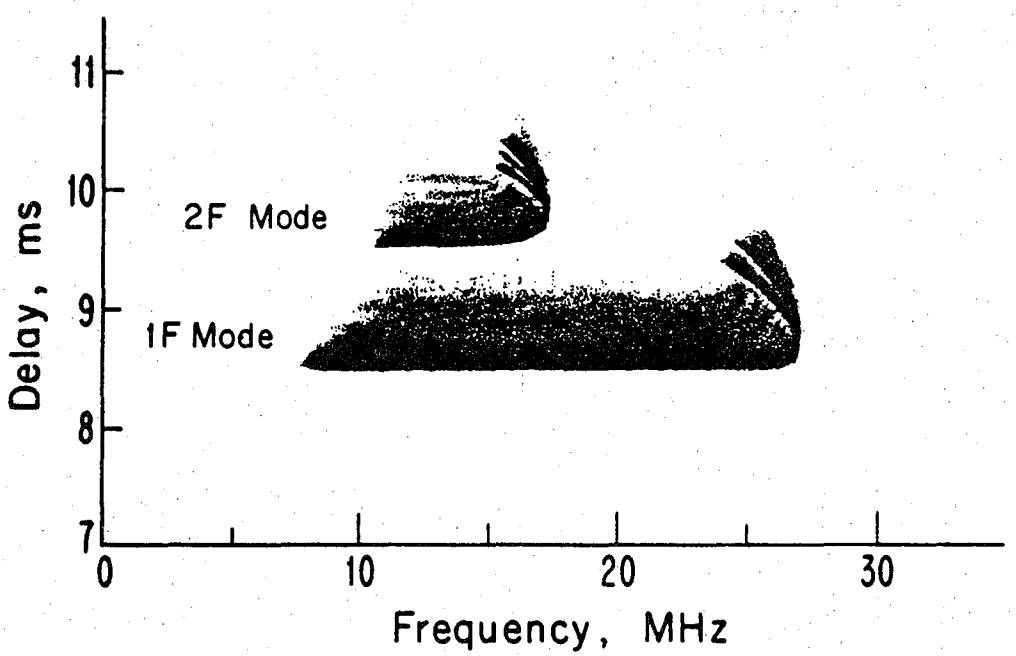

(b) SPREAD - F

Figure 5. Hypothetical ionograms.

figure. In Figure 5a, each propagation mode is essentially discrete in time. When turbulence is more severe or when adjacent modes become indistinguishable, a spread-F condition exists as shown in Figure 5b. When such conditions exist, the signal is not only spread more in frequency, but it is also spread in time. The time spread can be seen from the smear of each line of the ionogram in 5b. It is shown to be around 1 ms in this sample of 1F and 2F modes.

Systems, called sounders or ionosondes, are useful to determine the presence of ionospheric layers (Wright and Knecht, 1957; Agy et al., 1959; Watts and Davies, 1960; Balser and Smith, 1962; Evans, 1975; CCIR, 1982a). Depending on application, either vertical- or oblique-incidence sounders are used to transmit short pulses at different frequencies and to analyze the delays and amplitudes of their echoes. The generated plots of delay versus frequency are the previously introduced ionograms. A partial summary of ionogram terminology is given in Figure 6.

Several modes are present in this ionogram. However, the effective frequency range is limited between the lowest usable frequency (LUF) and the maximum usable frequency (MUF). Frequencies outside the range are lost through either total absorption or radiation that escapes into space. Within the LUF-MUF range, several familiar returns from E, F, or other layers are noted. The higher rays travel longer distances. They suffer longer delays. Furthermore, due to magneto-ionic interaction, individual modes may be split into two rays that traverse slightly different paths. These, the Ordinary (O) and Extraordinary (X) rays of Figure 6, appear different from those in Figure 5a. Usually, the more pronounced O-X splitting takes place at higher frequencies, such as near and just below the junction frequency (JF). The biggest signal distortion due to interference of delayed modes tends to occur when the delay spread between existing modes, often between the high and the low ray, is the largest (Salaman, 1962). This occurs at the so-called critical frequency (CF).

We shall use the term "intermodal multipath" to refer to multipath due to refraction from more than two layers in the ionosphere. The term "intramodal multipath" refers to multipath from a typically single ray that contains both ordinary and extraordinary magnetoionic components, or from the time-frequency spread of these components. Differential delay is the time difference between different propagation modes. Differential delay for intermodal multipath can be as long as 7 to 8 ms for long distance paths (Hoff and King, 1981), but more

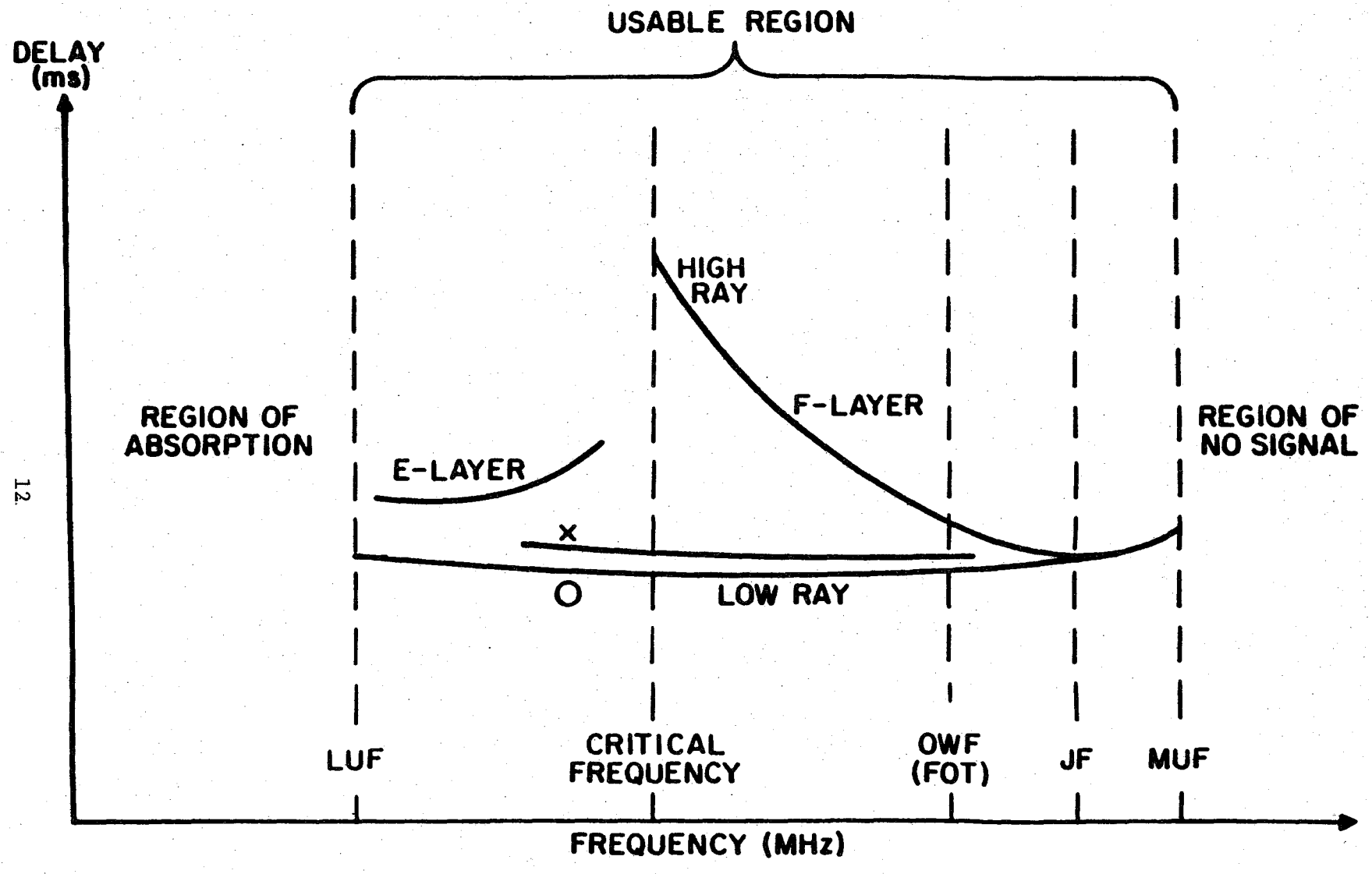

Figure 6. Ionogram terminology

commonly is 1 to 3 ms. The differential delay for intramodal multipath is of the order of ten's of microseconds.

Dispersion is the variation in the velocity of propagation of a wave with frequency. Watterson (1979) defines dispersion as being the negative derivative of the group time delay, τ, with respect to frequency. The slope of the appropriate mode/branch on an ionogram is a measure of the dispersive nature of a sky-wave link. As can be seen from Figures 5 and 6, the value of dispersion, i.e., the slope of the curve, is dependent upon the frequency. For purposes of estimating the dispersiveness of the channel, the well-behaved curve can be approximated by a series of straight-line segments. The spread or broadening of the curves can be viewed in a more complex, statistical manner. Agy et al. (1959) provides an atlas of many ionograms. The differences in these ionograms illustrate the point that the dispersiveness of the HF sky-wave channel is far from constant.

3. HF SPREAD SPECTRUM RADIO TECHNOLOGY

Spread spectrum technology has received considerable attention during the past few years. Numerous books and journal articles have been written on the subject (see for example Dixon, 1984; Simon et al., 1985; Chow et al., 1982; Cook et al., 1982; Cook and Marsh, 1983; Gerhardt and Dixon, 1977; Hoff and King, 1981; Holmes, 1982; Low and Waldstein, 1982; Milsom and Slator, 1982; Perry 1983a and 1983b; RCA, 1985; Salous, 1985; Skaug, 1981, 1982, 1984, and 1985; Thrower, 1978; and Tsui and Ibarki, 1982). The importance of spread spectrum technology to military communications is evident from the fact that an entire conference (1982 IEEE Military Communications Conference) was devoted to the subject. Many more references could be cited. The interested reader is referred to the cited references for a thorough treatment of the subject.

There are generally five types of spread spectrum systems:

- frequency hopping
- direct sequence
- time hopping
- linear frequency modulation (fm) or chirp
- hybrid systems.

Hybrid systems are those that utilize a combination of two or more of the first four technologies. Only the frequency hopping, direct sequence, and hybrid

systems will be discussed in this report because they are the technologies most commonly employed in, or contemplated for, HF communications systems.

3.1 Frequency Hopping HF Radio Technology

Frequency hopping (FH) technology is the technology most frequently used in spread spectrum HF communication systems. Numerous vendors have implemented, or are in the process of developing, frequency hopping HF radios.

We have not attempted to compile a detailed list of the characteristics of the radios available from various vendors. Some of the information is likely to be proprietary, while some information might be classified. However, we did investigate the following three key parameters:

- hopping rate
- instantaneous bandwidth
- frequency hopping range.

The practical frequency hopping rate appears to be an open question at this time. Hopping rates from 5 hops per second to 1000 hops per second or more are being discussed for sky-wave applications. As an extreme example, Milsom and Slator (1982) discuss a hop rate of 4000 hops per second. The state of the art of equipment technology and characteristics of the ionosphere both place constraints on practical frequency hopping rates. A reduction to less than 1000 hops per second may be warranted. This is discussed further in Sections 3.1.1 and 3.1.2.

The instantaneous bandwidth, i.e., the bandwidth for a single frequency dwell, is similar to that of nonhopping HF systems (e.g., 3-12 kHz). Wider bandwidths are being implemented in some hybrid systems as will be discussed in Section 3.3.

The frequency hop range of FH systems can conceivably cover the entire HF band (2-30 MHz). The ionosphere, however, places limits on the useful frequency hop range for a specified path, time of day, season of the year, and sunspot number. For example, circumstances may dictate a 3- to 10-MHz range at 0400 hr, a 7- to 20-MHz range at 1200 hr, and so on.

Two characteristics of sky-wave propagation that could limit the hop rate are

- differential delay
- fading rate of the channel.

The differential delay is also a concern to designers of frequency hopping spread spectrum systems. Consider a hop rate, H_r, of 1000 hops per second. The hop interval is given by

$$H_i = 1/H_r = 1/1000 = 1\text{ms}. \qquad (1)$$

If the differential delay is less than or equal to 8 ms, energy may be receive during each of the eight subsequent hop intervals. If the signal levels are of the same order of magnitude from each of the propagation modes contributing to this differential delay, the signal detection process may be difficult.

Milsom and Slator (1982) show that very high hop rates can be used to discriminate against intermodal multipath, but that this limits the FH range and the number of nonoverlapping hop frequencies. For discrimination of two paths having a differential delay of 250 μs, a hop rate of 4000 hops per second or faster must be used. If, however, the differential delay drops to less than 250 μs, one is led to the requirement that the hop rate be of the order of 10,000 hops per second to discriminate against intermodal multipath. These high hop rates may be difficult to achieve in practice because of hardware limitations. Of greater concern, perhaps, is the implication that the use of high hop rates leads to the elimination of the inherent diversity in the HF channel. By inherent diversity, we refer to the fact that when one propagation mode is in a down fade, a second mode may be in an up fade and hence deliver useful energy.

We conclude that the differential delay of the paths over which the system is to be operated restricts the frequency hopping rate to something of the order of 100 hops per second for long paths. For shorter paths, the delay spread may be as little as 2 ms. This would permit hop rates of 500 hops per second if delay spread were the only propagation consideration. That is not the case, however, in practice.

The HF channel cannot be characterized as being a mere additive white Gaussian noise channel. HF channels contain impulsive noise, both atmospheric and manmade; more about this will be presented in Section 4. Designers of HF systems, such as the Kineplex system, have long recognized the need to average the signal level for a period of time to reduce the effect of impulsive noise on the decision process. For this, plus other reasons, the Kineplex system uses the keying time of 13 ms. If one uses 13 ms as the hop interval for FH radios, the hop rate is found to be

$$H_r = 1/13 \text{ ms} \approx 77 \text{ hops/s}. \quad (2)$$

Of the two factors discussed in the foregoing paragraphs, the fade rate of the channel and the need to discriminate against impulsive noise causes the greatest limitation on the allowable hop rate of an FH system. Some researchers in the field claim that the maximum feasible hop rate may be as low as 5 hops per second for sky-wave HF communications (private communications with Mr. Les Morcerf, Litton Amecom, College Park, MD).

The hop rate, which is being incorporated into the present and future generations of frequency hopping radios, has direct impact on the process of defining requirements for a wideband HF channel simulator.

3.1.1 Hardware Constraints on Frequency Hopping HF Radio Systems

Two essential keys to the successful implementation of a frequency hopping HF radio are frequency synthesizers capable of rapid frequency changes and frequency agile antenna couplers. To prevent the loss of significant amounts of information, the switching and settling times of the frequency synthesizer should be less than 5 percent of the dwell time (Thrower, 1978). Thus, fast switching synthesizers are required. Faster hop rates can also be achieved by using two synthesizers. This allows one synthesizer to settle while the other is providing the output.

Much progress has been made in recent years in the design of frequency agile antenna couplers. Coupler tuning of the order of 300 μs has been achieved (see, for example RCA, 1985). This would permit hop rates of the order of 3000 hops per second.

3.1.2 Constraints on Surface-Wave Frequency Hopping HF Radio Systems

Frequency hopping HF radios developed for surface-wave application have the same hardware constraints as noted above for sky-wave systems. If one could assume that there is no unwanted sky-wave return mixed with the desired surface wave return, there would be no propagation-related constraints on the system. This may not always be the case, however, especially for systems that utilize nondirectional antennas.

3.2 Direct Sequence HF Radio Technology

There is current interest in the application of direct sequence (DS) spread spectrum technology to HF radio systems. The MITRE Corporation has investigated 1-MHz channels since 1968 (Belnap et al., 1968; Perry, 1983a and 1983b; Dhar and Perry, 1982; Low and Waldstein, 1982). The Naval Research Laboratory is currently making wideband (1-MHz) sky-wave propagation measurements using a channel probe (Wagner and Goldstein, 1982 and 1985; Wagner et al., 1983). Other channel probe measurements are being made using instrumentation having narrower bandwidths (100 kHz to 200 kHz). Haines and Weijers (1985) describe a channel probe that uses a 200 kHz spread spectrum waveform.

Despite the large interest in wideband, direct-sequence technology, there currently are no operational HF radios that have an instantaneous bandwidth of 100 kHz or more. The following sections contain a summary of the current research programs being conducted and a discussion of the system limitations due to both the ionospheric channel and hardware technology.

3.2.1 MITRE Wideband System

The MITRE Corporation has conducted experiments using a spread spectrum system having a 1-MHz bandwidth (Dhar and Perry, 1982; Low and Waldstein, 1982; Perry, 1983a and 1983b). The basic concept in their system is that the 1-MHz bandwidth can distinguish and therefore discriminate against intermodal multipath, and that the adaptive equalizer compensates for both the group delay dispersion and the fading due to intramodal multipath.

Figure 7 depicts the basic test configuration used by MITRE. The receiver operates in two modes: the sounder mode (i.e., the learning mode) and the normal communications mode. During the sounder mode, the equalizer is bypassed. A linear frequency modulated (LFM) probe signal is transmitted. Phase and amplitude measurements are made on each of 128 tones spaced by 8 kHz over a period of one second. These data are then used to calculate the tap gain coefficients in the equalizer.

Several equalizer algorithms have been developed by MITRE, including the inverse filter, matched filter, and Wiener filter (Dhar and Perry, 1982). Experimental data have been taken on a 1900-km path from Bedford, MA, to Eglin Air Force Base, FL. The inverse filter algorithm was used during these tests.

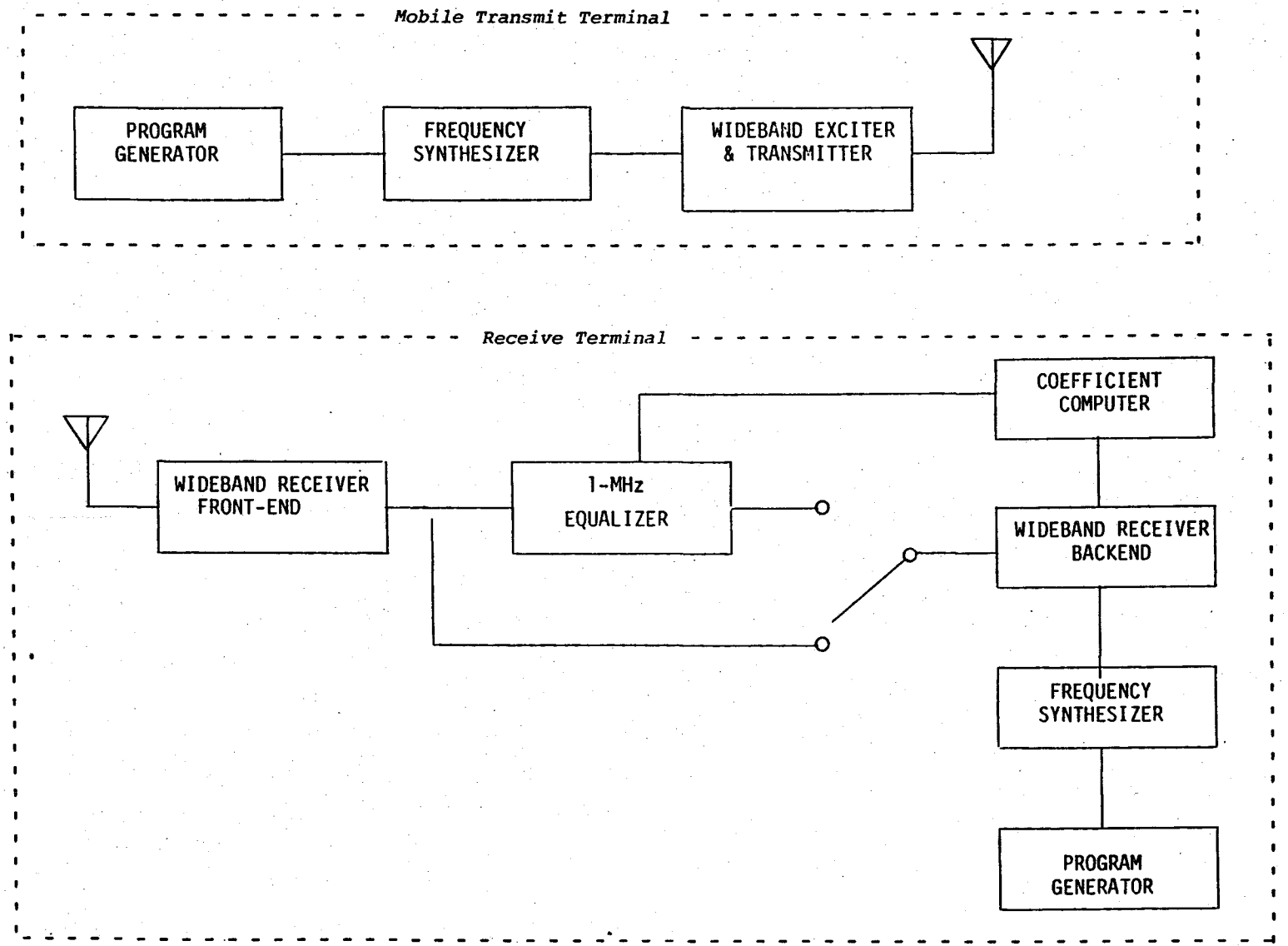

Figure 7. MITRE wideband HF communications test facility.

The observed propagation mode was primarily one-hop F layer. Results show that the equalizer was able to compensate for dispersion during the tests reported (Dhar and Perry, 1982). In a typical sample, the dispersion without equalization is 95 μs/MHz. With equalization it is 1 μs/MHz.

3.2.2 Other Research Programs

Experiments have also been conducted by the Norwegian Defense Research Establishment with a radio having a bandwidth up to 160 kHz (Skaug, 1981, 1982, 1984, and 1985). Skaug concludes that the performance of this radio was unacceptable when used in the 160-kHz mode, but was acceptable when used in the 80-kHz mode.

Tsui and Ibaraki (1982) claim that a transmitted spread bandwidth 20 to 30 times the coherence bandwidth of the channel can be used successfully. They describe a Delay Adaptive Combiner (DAC) receiver which uses adaptive equalization techniques to estimate adaptively and coherently combine unknown multipath delay spread pseudonoise (PN) signals prior to signal demodulation. Their work applies, in general, to any multipath/scatter channels. This includes HF sky-wave, troposcatter, and equatorial scintillation channels. The results they present are strictly theoretical, however, and are based on computer simulation rather than on actual measurements.

Milsom and Slator (1982) also present a theoretical treatment of the subject of the maximum spread bandwidth for HF sky-wave paths. They conclude that the spread bandwidth is likely to be restricted to about 100 kHz at night, with slightly larger bandwidths during the day. These results will be discussed further in the section that describes ionospheric effects on direct sequence systems.

Hoff and King (1981) discuss a Naval Ocean Systems Center (NOSC) program to develop signal processing techniques for spread spectrum HF systems. The NOSC approach was to (1) develop a wideband HF channel model and software simulator, (2) develop adaptive equalization signal processing techniques and computer simulation software, and (3) perform HF field tests to record signals for verifying the channel model and signal-processing algorithms. They designed an experimental decision feedback adaptive equalizer for a 100-kHz system. The reported results are encouraging. However, the channel model used

in the channel simulator was not validated using the field test measurements. These measurements were made using a system having a 96-kHz sounder mode.

Haines and Weijers (1985) discuss an HF communication system that has an embedded channel probe/sounder. The system is being used on a long transauroral path. Results of these measurements have not been reported.

Wagner et al. (1983) and Wagner and Goldstein (1985) have made measurements using a 1-MHz channel probe. Results of these measurements on a short (126 km) path are provided in the next section.

3.2.3 Sky-wave Propagation Constraints on Direct Sequence HF Radio Systems

Numerous authors have noted the ability of wideband systems to discriminate against multipath (see, for example, Price and Green, 1958; Turin, 1980; Chow et al., 1982; Salous, 1985; Hoff and King, 1981; Dixon, 1984, p. 275). In a direct sequence receiver, if a second signal is delayed by more than one code chip, the reflected signal is treated exactly the same as any other uncorrelated input signal. It, therefore, suffers suppression corresponding to the spread spectrum processing gain. Resolution of two paths requires that the signal bandwidth be larger than the reciprocal of the difference between the paths' delays. The differential delay spread between major modes is of the order of a few ms (up to a maximum of 7-8 ms for long paths). Thus, usual intermodal multipath can be resolved with relatively small bandwidths. Intramodal multipath resolution, however, requires much wider bandwidths. If, for example, the extraordinary and ordinary components are separated by 10 μs, a bandwidth of 100 kHz is required for their resolution.

Large signal bandwidths pose another problem for direct sequence HF sky-wave channels. The processing of direct sequence signals is performed coherently. The coherence bandwidth of HF sky-wave channels varies with time of day, season of the year, sunspot number, frequency, path length, and various ionospheric events. As will be shown, the coherent bandwidth is related to the dispersion of the channel.

Instead of a constant or linear model, Malaga (1985) proposes a quadratic model of the variation of delay as a function of frequency:

$$\tau_i(f) = \tau_{i0} + b_{i1}(f-f_0) + b_{i2}(f-f_0)^2 \qquad (3)$$

where: $\tau_i(f)$ is the delay at a frequency, f,
τ_{i0} is the delay at the center frequency, f_0,
b_{i1} and b_{i2} are constants that characterize the delay dispersion and interference pattern within the band of interest.

As noted earlier, dispersion is caused by the variation in the velocity of propagation of electromagnetic waves with frequency. The derivative of (3) with respect to frequency would yield the dispersion. However, Malaga provides no justification for the above equation, nor does he offer typical ranges or distributions of the parameters in (3).

For narrowband channels (less than 12 kHz) dispersion is negligible. Therefore, it has not been incorporated into any of the past and present narrowband HF channel simulators.

Table 1 presents some measured and predicted values of dispersion. Table 2 provides some measured coherent bandwidths. The measurements presented in those tables are the result of the use of the channel probes listed in Table 3.

The point of these tables is that there will be occasions when the dispersion will be greater than 100 μs/MHz. The coherent bandwidth will be 100 kHz or less at times. During those times, the ionosphere will degrade or restrict the operation of a direct sequence system.

3.3 Hybrid Spread Spectrum HF Radio Technology

Some spread spectrum HF radios are hybrids of frequency hopping and direct sequence technologies. These radios frequency hop at rates typical of radios that utilize only frequency hopping technology. For each frequency dwell, however, the transmitted signal uses direct sequence modulation. The instantaneous bandwidth of the direct sequence modulation is similar to that of conventional HF radios, i.e., 12 kHz or less. One hybrid radio has a somewhat larger direct sequence instantaneous bandwidth of 24 kHz (private conversation with Mr. Douglas Schmidt, Hughes Aircraft Corporation, Los Angeles, CA). There are no special known constraints associated with hybrid systems other than those that have been discussed in relation to frequency hopping or direct sequence systems.

Table 1. Measured and Predicted Values of Dispersion

Source	Conditions		Dispersion (μs/MHz)	Comments
Milsom and Slator (1982)	1F2/summer/926 km/SSN = 0 *		120 - 430	In each case the lower value corresponds to 70% of JF and the higher figure corresponds to 85% of JF. The values are predicted values.
	1F2/summer/926 km/SSN = 100		160 - 460	
	1F2/summer/2799 km/SSN = 0		20 - 45	
	1F2/summer/2799 km/SSN = 100		18 - 50	
	1F2/winter/926 km/SSN = 0		170 - 1000	
	1F2/winter/926 km/SSN = 100		530 - 1000	
	1F2/winter/2799 km/SSN = 0		27 - 30	
	1F2/winter/2799 km/SSN = 100		60 - 130	
Salous (1985)	1F2/spring/244 km	f_1 = 4.88-5.38 MHz	16	Dispersion was found by fitting straight line segments to half-megahertz sections of a measured ionogram.
		f_2 = 5.38-5.88 MHz	32	
		f_3 = 5.88-6.38 MHz	80	
		f_4 = 6.38-6.88 MHz	96	
		f_5 = 6.88-7.38 MHz	240	
		f_6 = 7.38-7.88 MHz	416	
		f_7 = 7.88-muf	656	
Wagner and Goldstein (1982)	1F2/fall morning/126 km		8 - 40	Swept frequency (2-30) MHz) channel probe was used. Extraordinary mode exhibited substantially less dispersion that the ordinary mode.

* Predicted sun spot numbers

Table 2. Coherent Bandwidths

Source	Coherent Bandwidth	Comments
Salous (1985)	100 - 150 kHz	Based on limited experimental measurements. A coherent bandwidth of 1 MHz was observed infrequently.
Wagner and Goldstein (1985)	100 - 200 kHz typical	Occasions when F2 layer extraordinary mode bandwidth has approached 1 MHz for brief periods.
Skaug (1981, 1982, 1984, and 1985)	80 kHz	For the particular path, a 160-kHz bandwidth was found to be noncoherent.
Milsom and Slator (1982)	100 kHz at night, slightly more in the daytime.	Maximum chip rate can be found from: $c_r = (a/\dot{\tau})^{1/2}$ where "a" can be found from Sunde (1961).

Table 3. Wideband Channel Probes

Organization	References	Bandwidth	Paths Measured	Comments
NRL	Wagner and Goldstein (1982) Wagner and Goldstein (1985) Wagner et al. (1983)	125 kHz 1 MHz	126-km path in California	NRL has plans for measurements on a 2300-km transauroral path.
NOSC	Hoff and King (1981)	96 kHz	232 km	
RADC	Haines and Weijers (1985)	200 kHz		
University of Birmingham	Salous (1985)	5 MHz	234-km path in England	1-MHz/second chirp sounder.
MITRE	Perry (1983a, 1983b) Dhar and Perry (1982)	1 MHz	2000-km path between Florida and Massachusetts	

One final advantage of hybrid systems over a pure frequency hopping radio is that discrimination against discrete multipath could be obtained even when using slow hopping (Milsom and Slator, 1982).

4. NOISE AND INTERFERENCE

Depending on their active element temperatures, all real signal receivers, detectors, and amplifiers generate certain amounts of thermal noise. Thermal noise has a uniform spectral density over a wide frequency range. Thermal noise exhibits Gaussian statistics when passed through all typically linear devices. Rather commonly this noise is called the additive white Gaussian noise (AWGN).

Gaussian noise exists in all narrowband and wideband HF radio systems. However, it is neither the only noise nor is it always the dominant additive disturbance. The receiving radio antenna is typically subjected to a group of natural and man-made noises or interferences. The relative intensities are illustrated in Figure 8.

In many sections of the globe, the dominant HF noise is usually man made (CCIR, 1982c). The man-made noise depends further on the siting of the radio receiver antenna. Urban locations are surrounded by a dense and varied population of electrical machinery and spark generating devices. They exhibit the highest relative intensity of man-made noise in the HF band. This intensity decreases more and more as one proceeds from core cities to smaller towns, to suburbia, and eventually to remote and unpopulated countryside.

Typically weaker than man-made noise sources are those of nature (CCIR, 1982b and 1983). Their intensity decreases gradually as one goes to higher radio frequencies. That is not always the case with atmospheric or thunderstorm generated noise. As shown, the atmospheric noise can be most severe at night and at the very lowest frequencies in the HF band. However, during daytime the situation tends to change. Peak atmospheric effects may be observed in the middle of the HF band, say around 15 MHz.

The statistical structure of the HF noises is generally far from Gaussian. The adjective "impulsive" has been coined to describe the high peaks in both man-made and atmospheric noise observations. Granted, nearly periodic noise waveforms of almost constant envelope have also been noted, especially when nearby repetitive emissions from automobile ignitions are passed through

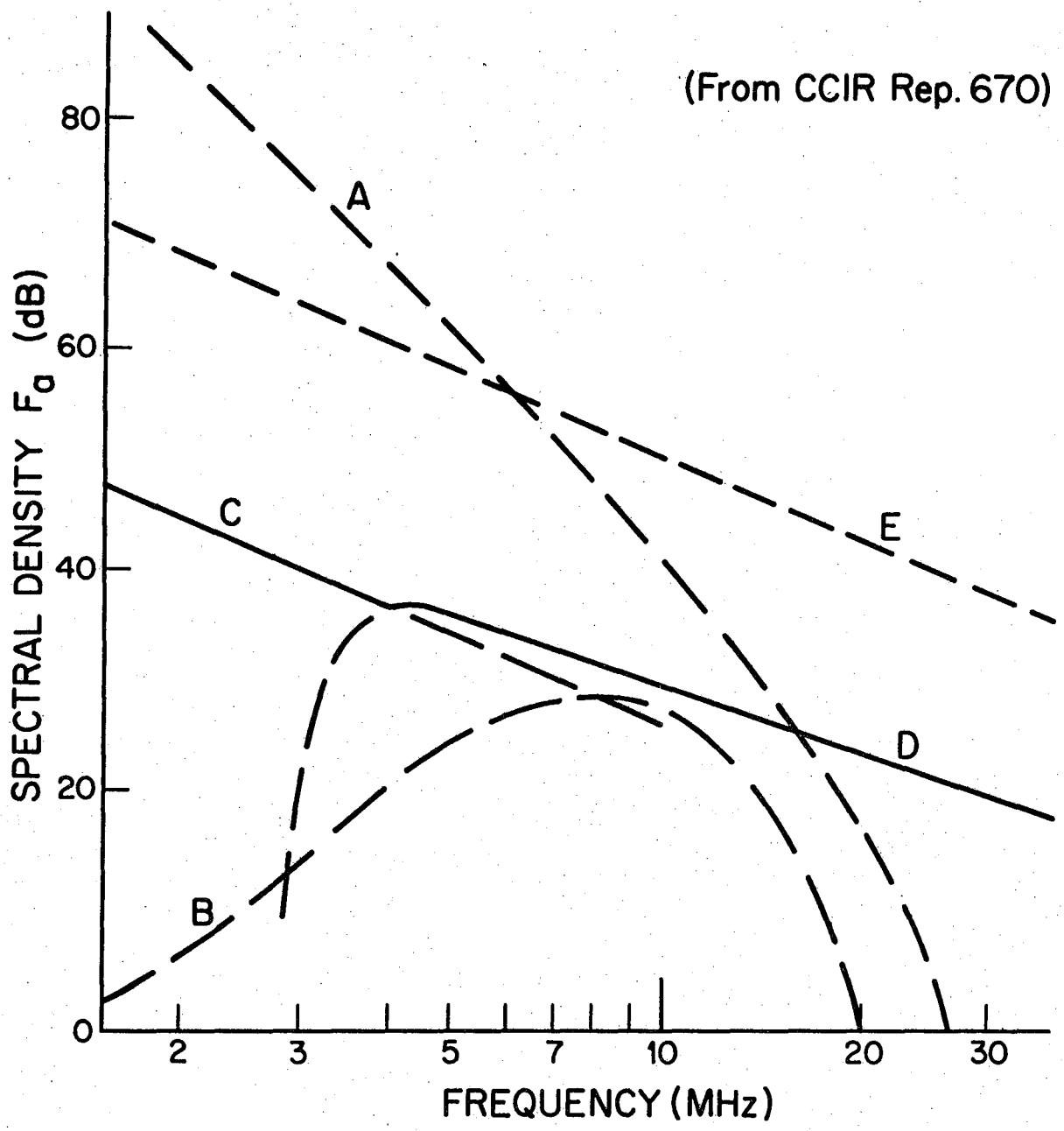

A: Atmospheric noise, value exceeded 0.5% of time.
B: Atmospheric noise, value exceeded 99.5% of time.
C: Man-made noise, quiet receiving site.
D: Galactic noise.
E: Median business area man-made noise.

Figure 8. Relative intensities of HF noise sources.

narrowband filters. However, the impulse characteristics are broadly considered to be more prevalent and of largest detriment to wideband systems.

On a rather global basis, noise measurements have been made in HF and other radio bands. The resultant statistical data have been summarized by CCIR in worldwide and regional noise maps and tables. Furthermore, modeling and simulation of these noises have been done and their effects have been analyzed (Coon et al., 1969; Bolton, 1971; Spaulding and Middleton, 1977).

The accepted, more or less standard, model for all dominant noise emissions in the HF band is a weighted sum of Gaussian plus impulsive processes. Classifications have been done to identify and to distinguish different mixes of the two components (Middleton, 1979a and 1979b). An example is shown in Figure 9. Two curves depict the noise envelope distributions of two man-made noise classes, the so-called Class A and Class B. Atmospheric noise is Class B. As indicated in the figure, both represent commonly occurring EM noise sources. One notes in Figure 9 that the Gaussian part is discerned on the right side of the graphs, where for probability levels in excess of 50 percent the plots follow straight lines with the same slope of minus one-half. The impulsive character is apparent on the left side. As seen, the impulse amplitudes can exceed quite high envelope levels but with very low probability.

Another additive disturbance is radio interference. It can be intentional or unintentional, local, or propagated as long a distance as the existing HF modes would permit. Jamming is an example of intended destructive interference. It may take the form of single-tone continuous wave (cw), high-power pulses, broadband modulated carrier, swept frequencies, or other intentionally harmful waveforms. Due to their unique nature, standardization of all interference--especially that of intentional interference--appears impossible. Interference should be modeled on a case-by-case basis.

5. NARROWBAND HF MODELS AND SIMULATORS

5.1 Modeling Background

In its simplest form, the Nyquist Sampling Theorem states that a signal band limited to B Hz does not suffer any distortion in the process of periodic sampling, provided that the sampling rate is larger than or equal to 2B per

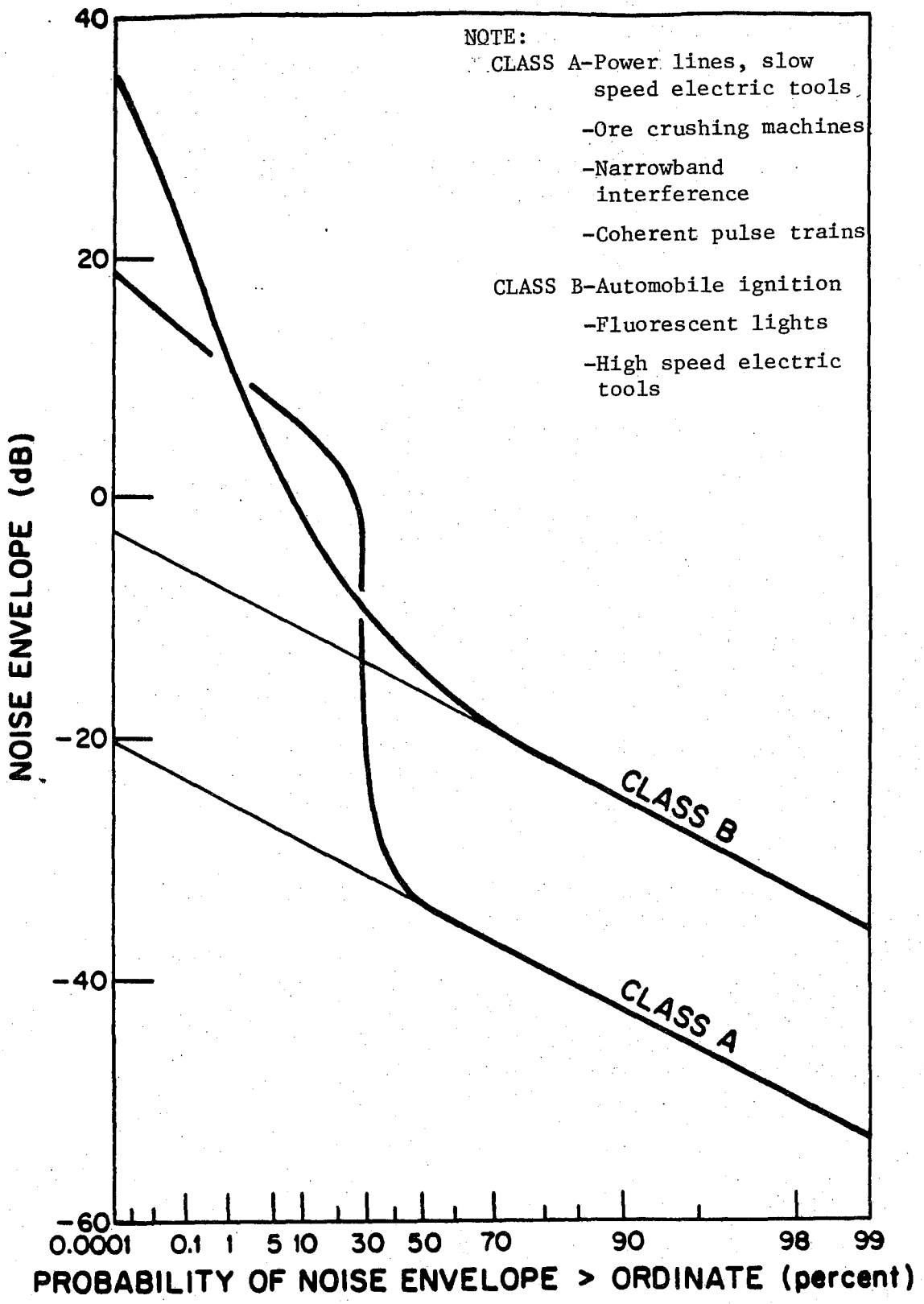

Figure 9. Classification of man-made noises.

second. The 2B rate is called the Nyquist rate or the minimum sampling rate. The spacing between samples or 1/2B is known as the Nyquist sampling interval.

Since in transmission and reception of narrowband signals one is clearly faced with band-limited representations of input and output signals, including the channel itself, the Sampling Theorem applies. This fact was fully recognized and utilized with appropriate enhancements a long time ago. The theoretical models for randomly time-varying HF channels and the concepts that led to the experimental RAKE system (Price and Green, 1958 and 1960) had their roots in the related Tapped Delay Line (TDL) channel model. An extremely primitive TDL channel model is given in Figure 10. The tap spacing, T, stands for 1/2B. There are n taps, n multipliers, and n multiplication constants (i.e., c_1, ..., c_n), in addition to the control and sum elements, plus the delay line itself. The magnitudes of n and T can be roughly estimated by simple rules of thumb. Assume, for example, that the bandwidth B should generously cover the standard voiceband. Hence let B=5 kHz. Accordingly, the TDL tap spacings are to be T=0.1 ms. It follows from the physical channel considerations, viz., the observed ionogram delay spreads, that the total length of the delay line may have to stretch over 10 ms. Consequently, the number of taps may have to be n=100. For many practical implementation schemes, such delay lines with one hundred or more taps are unrealistic. Thus, other approaches are needed even for this rather trivial narrowband example.

Fortunately, several effective modifications were promptly recognized. Their introduction culminated in sophisticated, yet also quite successful, theories, techniques, and systems (Di Toro, 1968; Belnap et al., 1968; Forney, 1972; Chase, 1976; Monsen, 1977; Watterson, 1979; Crozier et al., 1982; Perry, 1983a; Rappaport and Grieco, 1984). In telephony, the list of advances includes fixed linear and adaptive transversal equalization (Lucky, 1965; Gersho, 1969; Mueller and Spaulding, 1975; Qureshi, 1982). For general time-varying channels, there are the ultimate Kalman estimation techniques and the far more workable methods of Decision Feedback Equalization (DFE). See references (Walzman and Schwartz, 1973; Dentino et al., 1978; Belfiore and Park, 1979; Chang et al., 1980; Monsen, 1980; Crozier et al., 1982; Dhar and Perry, 1982; Aprille, 1983; Claasen and Mecklenbrauker, 1985). Last, but not least, there evolved several proposed and implemented models and simulators for the narrowband HF channels. Perhaps the most prominent among them is the ITS

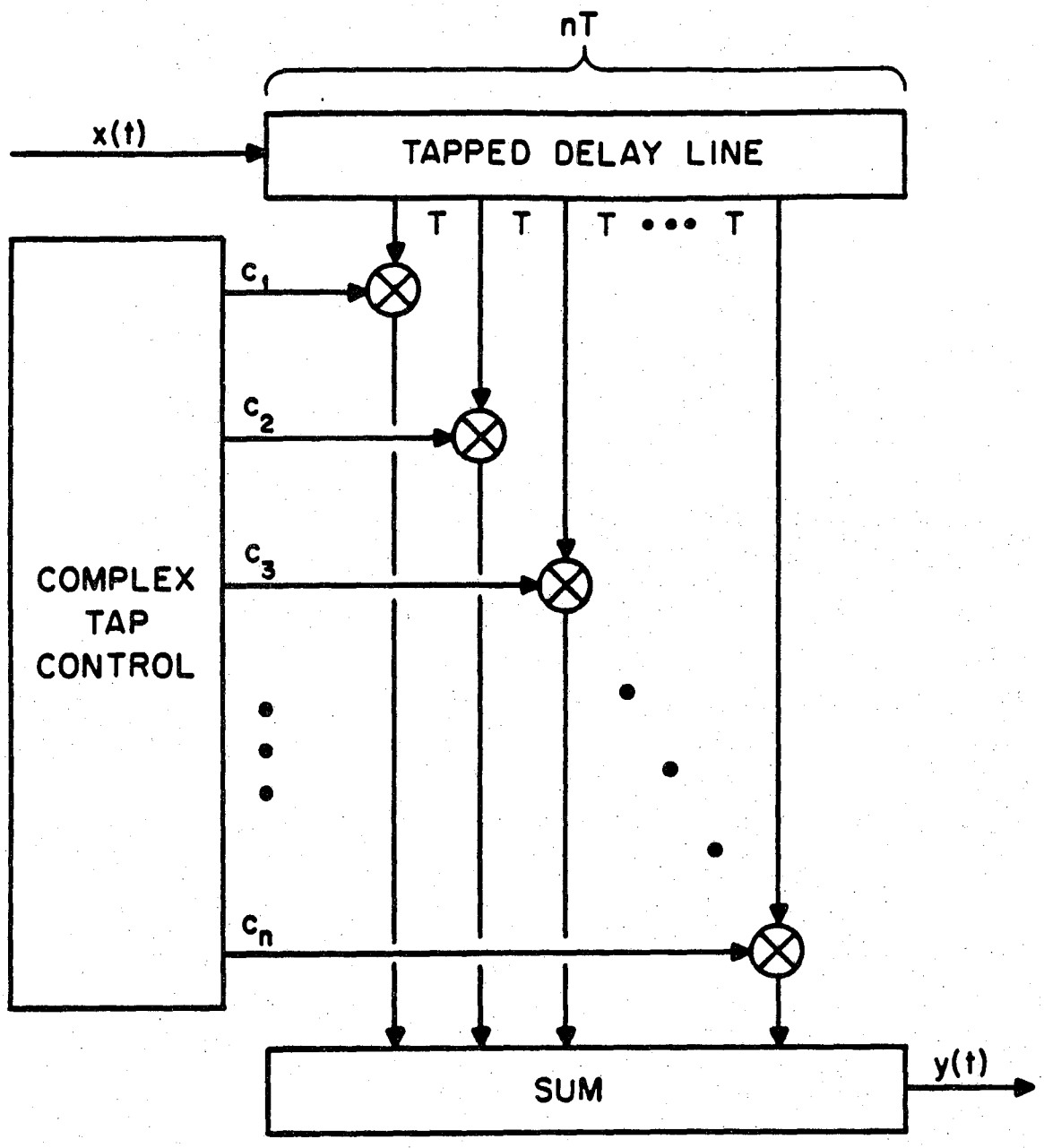

Figure 10. The basic tapped delay line model with equal tap spacing and constant multipliers.

or Watterson simulator (Watterson et al., 1969 and 1970). Both the Watterson model and machine will be the topic of Section 5.2.

Two advancements, quite pertinent to HF applications, are

1) the realization that a far smaller number of taps will often suffice, and

2) the replacement of the constant tap output multipliers with multiplier functions that somehow vary in time.

The concept of one so-modified TDL channel model is shown in Figure 11. There are three taps illustrated. In the earlier ionogram examples of Figures 5 and 6, they can correspond to the three modes observed, say, at frequencies just above the LUF. Thus, one can assign taps one-to-one for every HF propagation mode that contributes significantly to the received signal.

The purpose of the time-variant factors, $c_i(t)$, i=1,2,3, is to generate the t dependence in H(f,t). When a factor is a random function, its power spectrum exhibits Doppler shifts and spreads. Multiplied onto every tapped signal, these modal spectral distortions eventually appear in the summed output signal y(t). Single modes are also known to undergo delay distortions. If the delay characteristic of a mode is a rapidly changing function of frequency, one talks of it as the differential delay spread. In other instances, delay spreading may be due to some unresolved fine structure within the mode. In both cases, at a given radio frequency, signal energy can be variously dispersed (or scattered) in the time-frequency plane by selecting appropriate random multiplicand functions for the taps.

While the clear picture of the H(f,t) model (see Figure 11) is in front of us, some additional background terminology may be mentioned.

Being a random process in two independent variables, H(f,t) has only a limited region where it is significantly correlated. The region is usually depicted as a rectangle in the (t,f)-plane. Let its extent along the t-axis be t_d, and along the f-axis, f_d. Outside this rectangle or window, the values of H(f,t) are uncorrelated with the value observed in the center of the window. The two entities are called the correlation (or decorrelation) time and bandwidth, respectively. Their reciprocals, or more precisely,

$$\sigma_t = 1/2\pi t_d$$

and (4)

$$\sigma_f = 1/2\pi f_d,$$

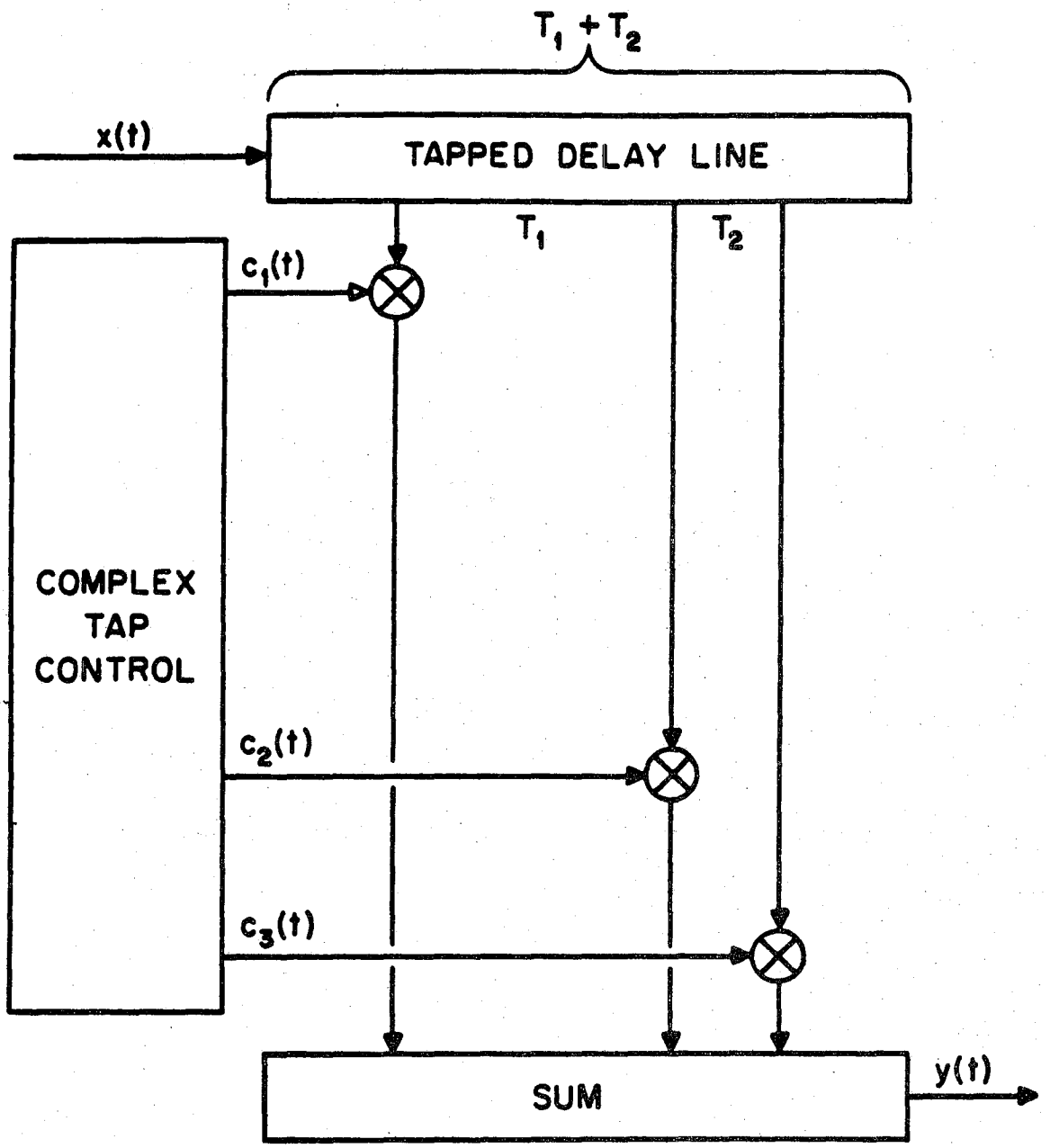

Figure 11. Modified tapped delay line model with few unequally spaced taps and variable multipliers.

are useful descriptors, known by several familiar names. Thus, σ_t has been occasionally called the Doppler, the Doppler spread, the fade rate, or even the fading bandwidth. For typical moderate HF paths, the values of the Doppler are of the order of 1 Hz. Its dual, σ_f, has been referred to as the multipath, the multipath spread or scatter, the delay spread, or some other measure of time dispersion. Assuming two or more modes, the typical range for the multipath spread is between 1 and 10 ms.

The product of the two sigmas defines a region in the time-frequency domain, over which significant portions of signal point energy may be scattered by the dispersive channel. As such, they reveal the main nonzero concentration of the so-called channel scattering function. This energy scattering function is the bivariate Fourier transform of the two-dimensional autocorrelation function of the time-varying filter response H(f,t). This brings one back to the channel correlation properties mentioned above.

5.2 Watterson Model and Simulator

Around 1970, the Institute for Telecommunication Sciences (ITS) developed an HF channel model, established the validity and the accuracy of the model in extensive field tests, implemented a corresponding HF channel simulator, and used the simulator to run laboratory performance tests on digital HF modems in a controlled and repeatable manner. Since the entire program was performed by C.C. Watterson and his colleagues (Watterson et al., 1969 and 1970; Watterson and Minister, 1975; Watterson, 1979), the model and the simulator are often called the Watterson model and Watterson simulator, respectively. Both the model and the simulator have been recommended by the CCIR for use in the performance evaluation of HF radios (CCIR, 1974). What follows is a brief summary of that model.

In principle, the channel model is a stationary realization of the unequal tap spaced TDL with time-function multipliers (see Figure 7). But, only the desired, delayed, and scattered signal is passed through the delay line. If, for instance, the propagation path is sufficiently short for the given radio frequency, the receiver may see a significant nonfading ground wave. The nonfading component is called specular to distinguish it from the fading scatter components that may or may not be present. Typical specular components

are the earliest to arrive at the receiver. In the model, therefore, they can be realized just before the signal enters the TDL. No TDL taps are involved. Specular components by themselves also undergo insignificant amounts of fade-related distortions. Therefore, a constant gain setting, instead of the complex, time-variable, function generators plus multipliers suffices for the specular component in the Watterson model.

Undesired signals, i.e., interference, also bypass the delay line, but may be subject to the time-function multiplicative effects. For sky-wave channels, the number of multipliers is nominally the same as the number of taps, also the same as the number of multipath modes, granted that the simulated receiver is to be of the nondiversity type. Any order or type of diversity is permitted by the model. However, only dual diversity has been fully implemented in the laboratory. This seems quite adequate for the majority of HF systems to be tested. If the number of available multipliers is fixed, the effect of the simplest dual diversity is to reduce the number of HF channel modes by two. Diversity combining techniques or related processing are not parts of the Watterson model. However, additive distortions consisting of AWGN and impulsive components are summed into the output. A block diagram of the channel simulator deployed for dual-space-diversity simulation is given in Figure 12.

From the narrowband channel characterization point of view, the most essential features are associated with the delay taps and their processing. The model assumes that, while the number of taps (i.e., modes) can be selected and their settings (i.e., delays, etc.) adjusted, this all must be done in preparation for a simulation run. During a run the settings remain fixed, as is required by stationarity. Similar statistical principles apply to the selection of the time-varying multipliers, called tap-gain functions by many. Then, however, based on experimental evidence and theoretical conclusions, a more complicated scenario emerges.

The key entities of the model are included in the following expression for the time-varying narrowband (NB) channel frequency response:

$$H(f,t) = \Sigma_i \, c_i(t) \exp(-j2\pi\tau_i f). \qquad (5)$$

Except for the O- and X-mode splitting, the sum Σ counts all, specular and scatter, multipath modes. The constant mode delays, τ_i, are included in the

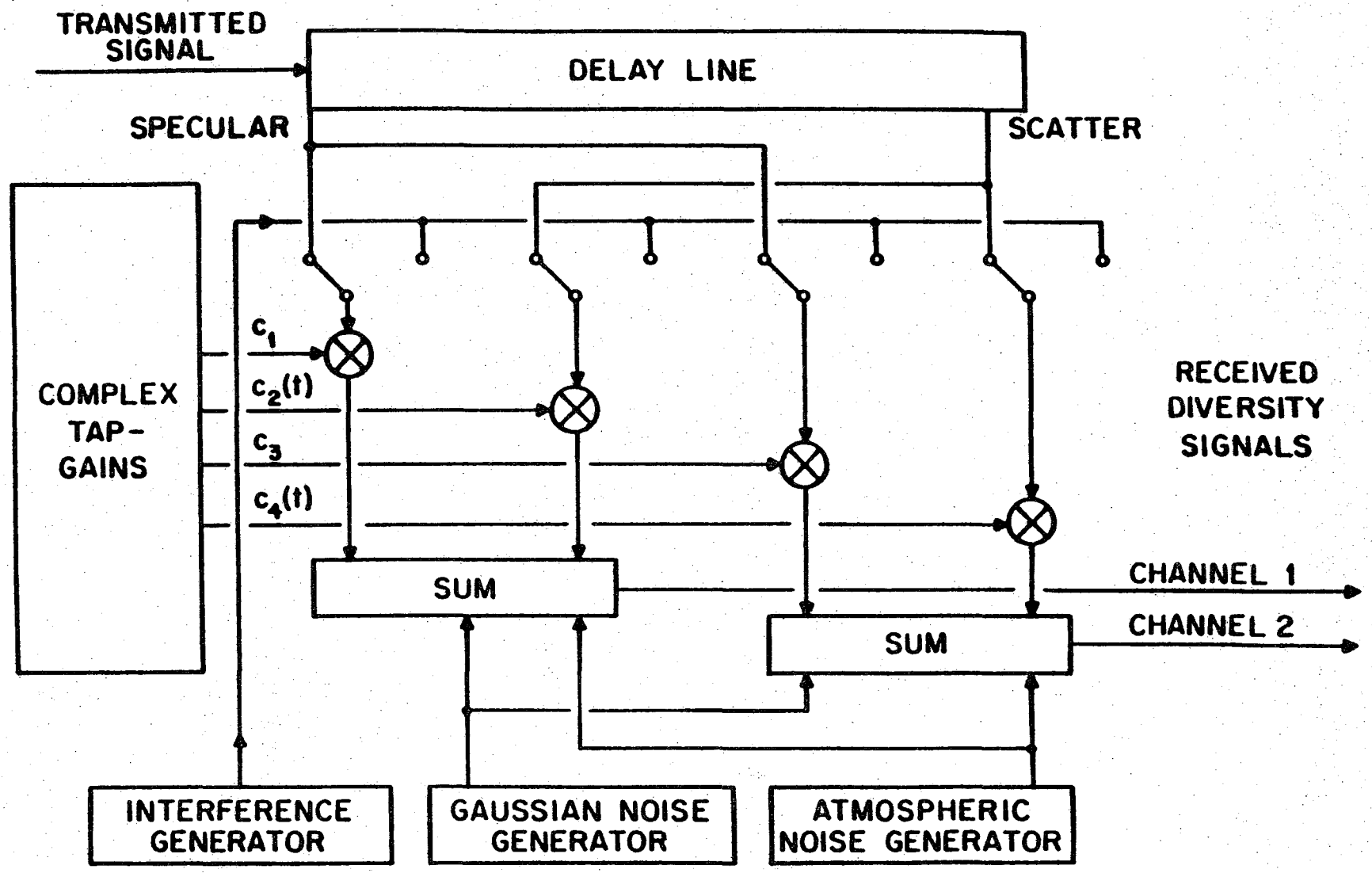

Figure 12. Block diagram for simulation of dual diversity reception of a ground- and sky-wave mix.

exponents and have the usual effect on frequency, f. The delays vanish for specular terms. Each tap-gain function, $c_i(t)$, is a complex function that applies uniformly (i.e., with constant first and second moments) over the entire channel bandwidth. Otherwise, however, it is a random function of time with certain preassigned, stationary, statistical properties. Specifically, each tap-gain function is an independent bivariate (complex) Gaussian function with zero mean and quadrature components that have identical rms values. In its effect on scatter mode amplitudes, such multiplicands cause independent Rayleigh fading.

Every tap-gain function, in general, is permitted to possess a double-peaked spectrum. The peaks represent the O-and-X ray splitting due to magneto-ionic effects (see Figures 5 and 6). The two spectra in question have Gaussian shapes with individually adjustable gains (amplitudes), and independent frequency shifts, as well as frequency spreads. The HF channel effects on the transmitted signal phase are thus determined by the total effects of the prescribed Gaussian processes. Of course, the rapidity of phase as well as amplitude fluctuations is also affected by channel bandwidth assignments. Typical bandwidth filter settings for this NB model range up to 12 kHz.

Table 4 is a summary specification of the numerical values available on Watterson HF simulator. It must be emphasized that the implementation of this laboratory, test instrument represents conservative, moderately practical, state of the art engineering, circa 1970. Today, for fewer resources, more can be procured in terms of parameter ranges, accuracy, and other overall measures of performance. Many parameter inaccuracies listed in Table 4 are probably extremes in that they are deduced from estimated largest possible equipment errors. The specular and scatter path attenuations, in decibels, have the indicated accuracies over the range normally used. Listed deviation bounds, for attenuations and other parameters, do not include variations external to the simulator.

Proceeding from the top down in Watterson's simulator specification, one finds first the three standard options for bandwidth. They are 3, 6, and 12 kHz, respectively. The maximum number of paths (viz., modes or taps) is four. The delay settings for taps are selectable constant values in 20-μs steps over a quite realistic interval from 0 to 10 ms. Note that this would normally exclude frequency-dependent delays and associated differential-delay

Table 4. Watterson's Channel Simulator Specifications

Parameter	Available Values	Accuracy
Bandwidth, B	3, 6, or 12 kHz	--
Number of Paths, n	4 maximum	--
Delay, τ_i	0 to 10 ms in 20-μs steps	0.5 μs
Dispersion, D_i	0, -100, -220, and -320 μs/kHz	2×10^{-2}
Specular Atten., $\bar{A}_i$	0 to 100 dB continuous	0.2 dB†
Specular Phase, $\bar{\theta}_i$	continuous (modulo 2π)	0.01 rad.
Scatter Atten., $\tilde{A}_i$	0 to 100 dB continuous	0.2 dB†
Frequency shift, ν_i	Int. Synthesizer: 0, ±1, ±2, or ±5 x .01, .1, 1, 10, or 100 Hz	1×10^{-4}
	Ext. Synthesizer: -500 to 500 Hz in 1-mHz steps	1×10^{-6}
Frequency Spread, $2\sigma_i$	Each Path: 1, 2, or 5 x .01, .1, 1, 10, or 100 Hz	2×10^{-2}
	One Path: 1.00, 1.33, 1.78, 2.37, 3.16, 4.22, 5.67, or 7.50 x .01, .1, 1, 10, or 100 Hz	2×10^{-2}
Fading Spectrum, $v_i(\nu)$	3-pole approximation of Gaussian	<0.03 dB*
Signal to Noise, E_b/N_d	-100 to +90 dB continuous, Gauss. Atmos.	0.2 dB† 0.5 dB†
Atmospheric Noise Impulsiveness, V_d	HF: 7.2 dB in 2.7 kHz LF: 10.8 dB in 2.7 kHz LF: 9.0 dB in 2.7 kHz	-- -- --
Signal to Interf., S/I	-100 to +90 dB continuous	0.2 dB†
Space Diversity	Single or independent dual	--
Internal Distortions: Additive Nonlinear	 < -70 dB relative to signal+noise < -70 dB relative to signal+noise	 -- --

†Over range of significance *Theoretical

spreads. The latter is acceptable for narrowband HF simulation because dispersion has been shown to be negligible for such channels. However, to extend the simulator's use to highly dispersive media such as VLF/LF channels, dispersion filters are available to the signal paths between delay line taps and corresponding path gain multipliers. The dispersion filters are all-pass filters with a delay characteristic linear in frequency. By switching to different delay slopes, one selects from the available dispersion numbers. Again, note that these are constant settings, entirely independent of frequency.

By going down row-by-row in Table 4, one finds numerical specification for the previously introduced parameters of the model. A more detailed explanation of their features appears unnecessary here. Interested readers will find comprehensive descriptions in the extensive list of references (Section 9). However, one may note that the model admits both Gaussian and atmospheric noises at continuously preset signal-to-noise ratios, and with controlled impulsiveness coefficients. Likewise, the model permits exterior signal interference at fixed signal-to-interference levels. At the very bottom of the table, one finds two possible internal distortion sources, both less than -70 dB relative to the signal-to-noise ratio. They appear to be due to A/D conversion and occasional clipping. However, -70 dB appears so minute compared with ordinary HF fluctuations as to render their detrimental effect entirely negligible.

5.3 Other Simulators

In conclusion of this section, it should be acknowledged that numerous other models as well as other simulators have been developed. Most, if not all, of them are elaborated in the literature (Adams and Klein, 1967; Bussgang et al., 1974; Raut, 1980; Signatron, 1980; Ehrman et al., 1982; Ehrman, 1984). We will not review them extensively because 1) their capabilities are not superior to those of the Watterson scheme, 2) they are all narrowband, 3) all parameter settings noted are constant versus frequency, and 4) the other models are apparently not as well experimentally validated and documented as is the Watterson model.

Other simulators have been built based on the Watterson/CCIR HF channel model. One notable example is the HF channel simulator built by Signatron, Inc. (Ehrman et al., 1982). A functional block diagram of the Signatron system

is provided in Figure 13. Although both are based on the same channel model, the Signatron simulator implementation is quite different from the ITS simulator implementation. The Signatron simulator uses an array processor to implement the model in software, whereas the ITS simulator is a hardware implementation of the model. Both can be used to evaluate the performance of HF radios. The Signatron simulator performs an A/D conversion on the output of the HF transmitter (either baseband or rf). After digital filtering, the digital bit stream is fed into the array processor which distorts the signal using the model algorithms specified by the Watterson/CCIR model. Three paths, each having an ordinary and an extraordinary component, are simulated. The paths are summed with both Gaussian and impulsive noise. The summed digital output is filtered and converted to an analog output. This output is then input into the receive section of the HF radio under test.

The bandwidth of the Signatron simulator was originally 4 kHz, but has been recently extended to 12 kHz (Ehrman, 1984).

5.4 Model Validation

Even for narrowband HF channels, the verification of a given model's validity or accuracy of fit is considered important for reliable operation of ordinary data transmission. When faced with more advanced systems, especially those with designs or algorithms that depend on proposed channel simulation, the question grows in significance. After all, the substantial advantages promised by laboratory simulator tests over on-the-air experiments may be entirely erroneous, unless it is ascertained how accurately the model (on which the simulator implementation is based) represents the real HF. While many measurements of the ionospheric channels, such as the aforementioned ionogram generating sounders, have been made over the last 50 years, many detailed properties were not available before the work of Watterson. Consequently, the real accuracy and validity of any past models and simulators can be questioned, especially if they are to be used outside their proposed immediate application.

In this section we talk mostly about the experimental verification of Watterson's ionospheric channel model. However, there are a few general comments to be noted. First, long experience on actual links and understanding of propagation physics have led to HF prediction programs (Lucas and Haydon, 1966; Haydon et al., 1969; Haydon et al., 1976; Teters et al., 1983). Given

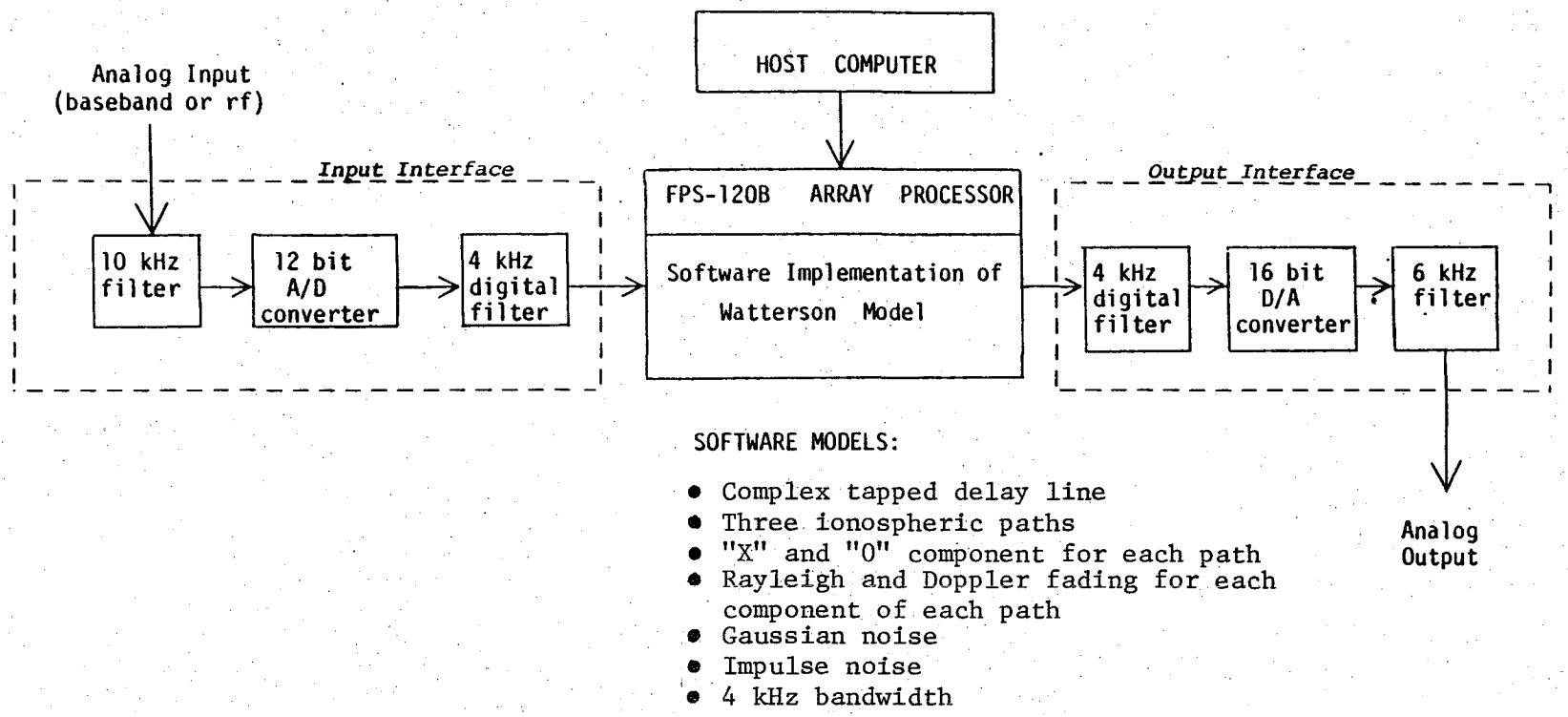

Figure 13. Signatron implementation of the Waterson/CCIR model.

path geography, time of day, solar activity, and other factors, these services forecast best working frequencies, their percentage availability, as well as some performance aspects. Published CCIR Reports support their use. Second, the usual ionograms also tend to help when they are current and available. They reveal what frequencies are useful at a certain time, over a certain path. As with most field tests, sounding tends to produce data that one inevitably associates with typical conditions. It may involve long waiting times to catch all or even a few atypical events in one HF setup, when they might occur rather commonly elsewhere. Therefore, things like sudden ionospheric disturbances (SID) present a problem. They occur when least expected. Relative delays are easily obtained from ionograms. However, the ordinary ionograms show little or no further detail. For instance, seldom if ever is one in a position to deduce from ionograms individual mode amplitudes, phases, time dispersions, Doppler shifts, Doppler spreads, etc., not to mention mutual statistical dependence between observables.

The model verification experiments by Watterson took place in November of 1967 (Watterson et al., 1969 and 1970). They were preceded by preparation and testing of the equipment to support test bandwidths of 12 kHz or higher. The transmitting system was installed at Long Branch, IL (40°13'N, 90°01'W). The receiver was located in Boulder, CO (40°08'N, 105°14'W). The propagation path has a great-circle distance of 1,294 km. It is at a very moderate latitude and displays a nearly perfect East-to-West orientation. Two assigned frequencies of 5.864 MHz and 9.259 MHz were used for night and daytime operation, respectively. In both cases, the rf was sufficiently below the predicted MUF to make it likely that both one- and two-hop modes would be present.

The link was operated continuously in three separate test periods. Over 7 hours of recorded measurements were obtained at night (5.864 MHz) and nearly 10 hours during daytime (9.259 MHz). The recorded data were subsequently sampled, reduced, processed, and analyzed with verification of the proposed channel model being the main objective.

Data were divided into 10- to 13-minute intervals called samples. Of all the samples covering the total 17 hours of measurement, about 2 hours or 12 percent were found to be approximately stationary in terms of fading rates, modal time delays, and average powers in the modes. Three particular sample

intervals, designated as I1, I2, and I3 by Watterson, received the most detailed analysis. The following key results and conclusions were obtained from these samples.

A summary of the samples is offered in Table 5. Note that the number of distinct modes, excluding the magneto-ionic or O-X fine structure, is either 3 or 4. In all cases the channel delay numbers remain under 1 ms, which is quite normal. The Doppler shifts and spreads are also well behaved. Their magnitudes are small fractions of a hertz. The so-called path time spread, which measures the effective delay smear within a mode, is observed to range from 20 to 100 μs. As claimed in the literature and verified by Watterson, this leads to definite conclusions about the maximum bandwidth over which the model is an accurate replication of the real channel behavior. This "validity bandwidth" for the model is not a fixed, forever invariant, entity on an HF circuit. The last row of Table 5 reveals that all three samples have markedly different validity bandwidths. However, the overall conclusion is still positive. For narrowband applications, the model offers a reasonable facsimile of the real thing.

Moreover, further analysis shows that the tap-gain functions are justified as defined. It is indeed valid to infer them as mutually statistically independent, complex (bivariate) Gaussian random processes at baseband. Their spectral densities are also representable as claimed. They are either single, or sums of two, Gaussian functions. To fit observations, these Gaussian peaks must be permitted arbitrary central positions and different spreads.

Perhaps the most noteworthy conclusion drawn from these validation tests is that under the assumed narrowband conditions certain parameters are indeed constants for workable intervals of time and over all frequencies in the band. This includes modal structures, i.e., number of modes and their O-X splits, constant mode delays, constant mode amplitudes, delay spreads, Doppler shifts and spreads, and the total amount of mode dispersion, to mention the main variables. It is proper to assign to them constant numeric values over bandwidths that do not exceed 12 kHz for daytime sky-wave links and a smaller bandwidth for nighttime operation. However, to presume constant values for larger bands appears unjustified. A look at the wideband properties of ionograms only strengthens this suspicion.

Table 5. Summary of the Three Samples

SAMPLE	I1	I2	I3
Frequency (MHz)	9.259	9.259	5.864
Number of Modes	3	4	3
Channel Time Delay (μs)	137	173	589
Channel Time Spread (μs)	478	520	464
Channel Doppler Shift (Hz)	.0013	.0171	.110
Channel Doppler Spread (Hz)	.123	.140	.0666
Path Time Spread (μs)	20	30	100
Validity Bandwidth for the Model (kHz)	12.5	8.3	2.5

In the conclusion of this validation section, Tables 6, 7, and 8 are presented. They show how the summary numbers of Table 5 were derived for the three sample intervals, and how they may relate to modal details of four prime parameters. In Tables 6, 7, and 8, these four parameters are relative mode power, its time delay, Doppler shift, and Doppler spread. Given the defined units of measurement, the four numerical values constitute a 4-tuple "parameter vector" in the tables.

As an illustration, consider sample I1. Table 6 states that the signal is observed to have three modes: E, F, and 2F. By convention, the total channel power is said to be unity or 0 dB. Depending on the experimental arrangement, that total power can be determined directly or by adding relative powers received over individual paths. The normalized powers in the three modes shown are

-1.2 dB or .763 in mode E,

-7.2 dB or .192 in mode F,

-13.5 dB or .045 in mode 2F.

Mode E is seen to be split further into ordinary and extraordinary components. Their respective relative powers are

-4.1 dB or .390 for component O,

-4.3 dB or .373 for component X.

The remaining three quantities, namely the time delay and the Doppler shift and spread, have different values over different propagation paths. To combine the three distinct modes into a single effective number for the combined multipath channel, a weighted sum is used for the channel parameters. The weights are the same relative normalized powers noted above. Thus, for the total Doppler shift in Table 6, one obtains

.763 (.0094) + .192 (.0089) + .045 (-.167) = .0013 Hz.

Similar calculations are performed for all four parameters and over all modes observed in data samples I1, I2, and I3.

6. WIDEBAND HF MODELING

6.1 Hypothetical Approach

The extension of narrowband (e.g., 10 kHz) channel models to wideband (e.g., 2 MHz) models cannot be substantiated by comprehensive measured data at this time. Nevertheless, this section does attempt to present an approach to

Table 6. Detail for Sample I1

Parameter Vector	Channel	Mode	O-X Split
		E	-4.1 40 .0022 .0073
		-1.2 40 .0094 .0272	
Rel. Power (dB)	0*		-4.3 40 .0170 .0318
Time Delay (μs)	137		
Doppler Shift (Hz)	.0013		
Doppler Spread (Hz)	.123	F	-7.2 290 .0089 .144
		2F	-13.5 1139 -.167 .340

* By Convention

Table 7. Detail for Sample I2

Parameter Vector	Channel	Mode	0-X Split
		E	
			-4.1
			40
			.0008
		-1.7	.0064
		40	
		.0071	
		.0153	-5.5
			40
Rel. Power (dB)	0		.0127
			.0084
Time Delay (μs)	173		
		F	
Doppler Shift (Hz)	.0171	-5.9	
		290	
Doppler Spread (Hz)	.140	.0159	
		.180	
		M	
		-17.6	
		590	
		.108	
		.334	
		2F	
		-12.6	
		1126	
		.118	
		.336	

Table 8. Detail for Sample I3

Parameter Vector	Channel	Mode	O-X Split
		*	
			-3.8
			445
			.0764
		-1.6	.0360
		445	
		.0989	
		.0658	-5.7
			445
			.134
			.0320
		*	
			-10.8
Rel. Power (dB)	0		750
			.121
Time Delay (μs)	589	-7.7	.0104
		750	
Doppler Shift (Hz)	.110	.131	
		.0229	-10.6
Doppler Spread (Hz)	.0666		750
			.141
			.0130
		*	
			-12.9
			1088
			.121
		-8.5	.0149
		1088	
		.140	
		.0335	-10.4
			1088
			.140
			.0206

* Unidentified

WB/HF modeling. Based on extrapolation of past NB results, more than on the latest wide bandwidth measurements (Wagner and Goldstein, 1982 and 1985; Wagner et al., 1983) or other pertinent inferences, the approach is more conjectural than factual. More questions are asked than answered. Issues are raised, but hardly settled.

The HF channel is not stationary over a very long time. For the NB simulator, Watterson's tests established a 10-to 15-minute window of apparent stationarity. What happens when the band is much wider is not too certain. However, one should expect no novel nonstationarity effects here. For 10 to 15 minutes, or thereabouts, the wideband channel structure is likely to be more or less fixed. By that one means that over the entire bandwidth of interest the number of modes, their amplitudes, their delays, Doppler spreads, and so on, retain constant profiles as functions of frequency. The situation is as illustrated in Figure 14. Over a sufficiently long sky-wave path, ionograms are observed at several 3-hour instances. When scrutinized, they show quite discernible differences from one snapshot to the next. The operating frequencies increase as the morning hours pass. The number of modes undergo changes. If one focuses only on 15 MHz, one finds no modes at 0300 and 0600 hours, five modes at 0900, and two at 1200 hours. The intermode delays are on the order of 1 ms, but their systems effects are unclear because the relative amplitudes, Dopplers, etc., are unresolved by simple ionograms like those shown in Figure 14. Assuming further resolution in these ionograms, it is postulated that the above stationarity window still remains valid.

What can the higher resolution probe hope to reveal about the WB channel? The answer comes in many forms. For example, Figure 15 is based on the premise that the channel bandwidth is 2 MHz, but that depending on the time of day different 2-MHz slots are utilized. In said slots, the multipath modes display a fine structure of rf energy (viz., amplitude) scatter versus delay that, because of Figure 14, must somehow vary with frequency. The amplitudes and widths of the encountered distributions vary. Some modes expire in the middle of the band, others stretch across the band, while yet others merge or split apart at certain junction frequencies. But this is far from being the whole story. The previously mentioned Doppler effects must also be included, as must be a large matrix of mutual cross-correlations between all the above random processes or variables, as the case may be. Things would be greatly simplified

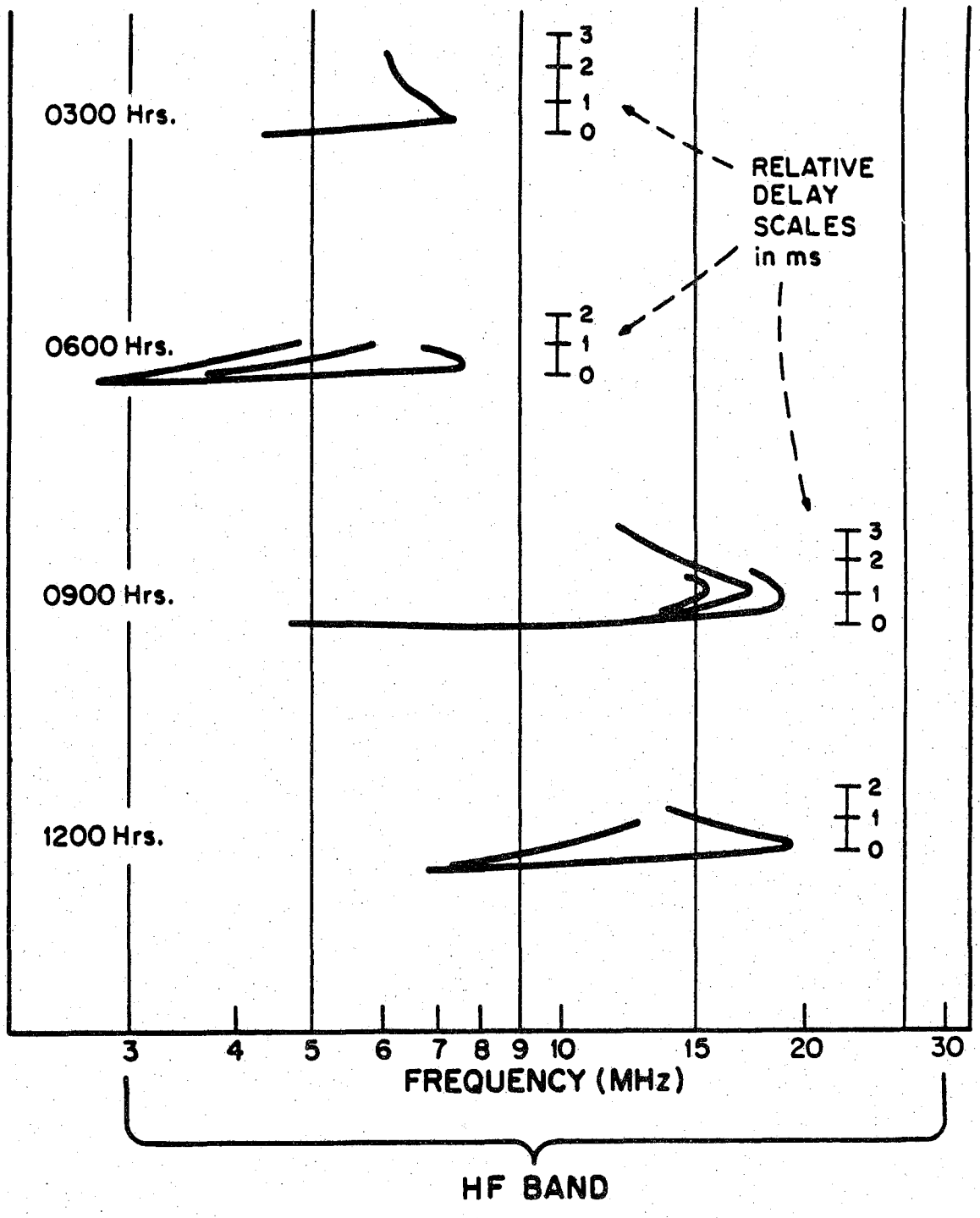

Figure 14. Ionogram snapshots of multipath variation over time and wide bandwidth.

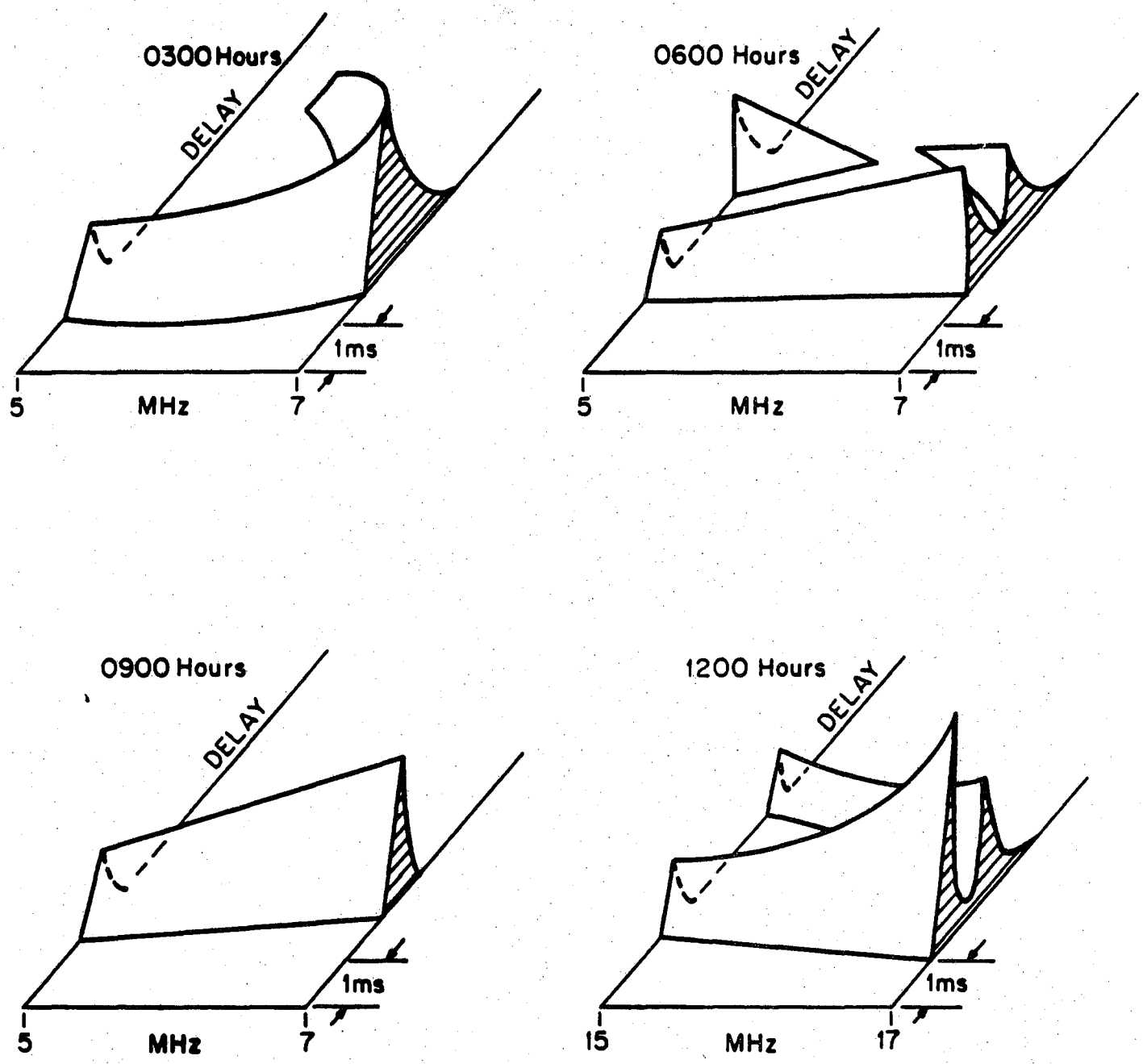

Figure 15. Relative amplitudes and delay scatter in a 2-MHz bandwidth.

if most of the entities turned out to be statistically mutually independent. However, there appears to be a genuine shortage of experimental data on this issue. And one doubts whether significant independence (or even approximate uncorrelation) could be realistic from the wave propagation point of view over so large bandwidths of concern.

Let us return to experimental results. Figure 16 shows an oblique incidence ionogram observed July 16, 1957, at 2054 hr (CST), over a moderately long west-to-east path. More precisely, the transmitter was in Boulder, CO; the receiver was in Sterling, VA. That represents a surface distance of 2370 km or roughly 1470 miles. The corresponding ground-wave delay should have been around 7.90 ms. But, of course, due to the long-distance surface-wave attenuation, no ground-wave mode was noted. Instead, Figure 16 contains six sky-wave modes. The modes are numbered 1 through 6, with circled numerals, and so ordered that smaller numbers would correspond to the shorter signal delays. The very least delay of 8.28 ms is equivalent to a free-space path length of slightly less than 2500 km. The largest delay of 9.24 ms would be caused by a distance of almost 2800 km. Between the extremes one has a chance of finding at least one signal mode, as long as the rf is not less than 4 MHz nor more than 18 MHz.

Consider modes 1, 2, 4, and 5. They all meet at the frequency of 18 MHz, which is both their JF and the MUF for the channel. At this juncture, the slope of the delay characteristic is infinite. By definition, that amounts to an unbounded delay dispersion in the HF channel. How it should be handled in the model (or in the simulator) is far from clear. In Figure 16 the matter is artificially "resolved" by deleting the bothersome point (see the horizontal cut). The cut separates the four incident modes from each other.

In principle and consistent with Watterson's model, one can assume that a single TDL tap be dedicated to each of the six modes, appropriately placed on a delay line of wide enough (!) bandwidth. But that is only part of the problem. The six delay curves in Figure 16 are nonlinear functions of frequency, whereas the fixed taps represent constants. To clarify the time-varying channel transfer function, H(f,t), for this and similar ionogram cases, from now on we propose the following wideband (WB) channel model:

$$H(f,t) = \Sigma_i \, A_i(f) \, u_i(f,t) \, \exp[-j2\pi\tau_i(f)f]. \qquad (6)$$

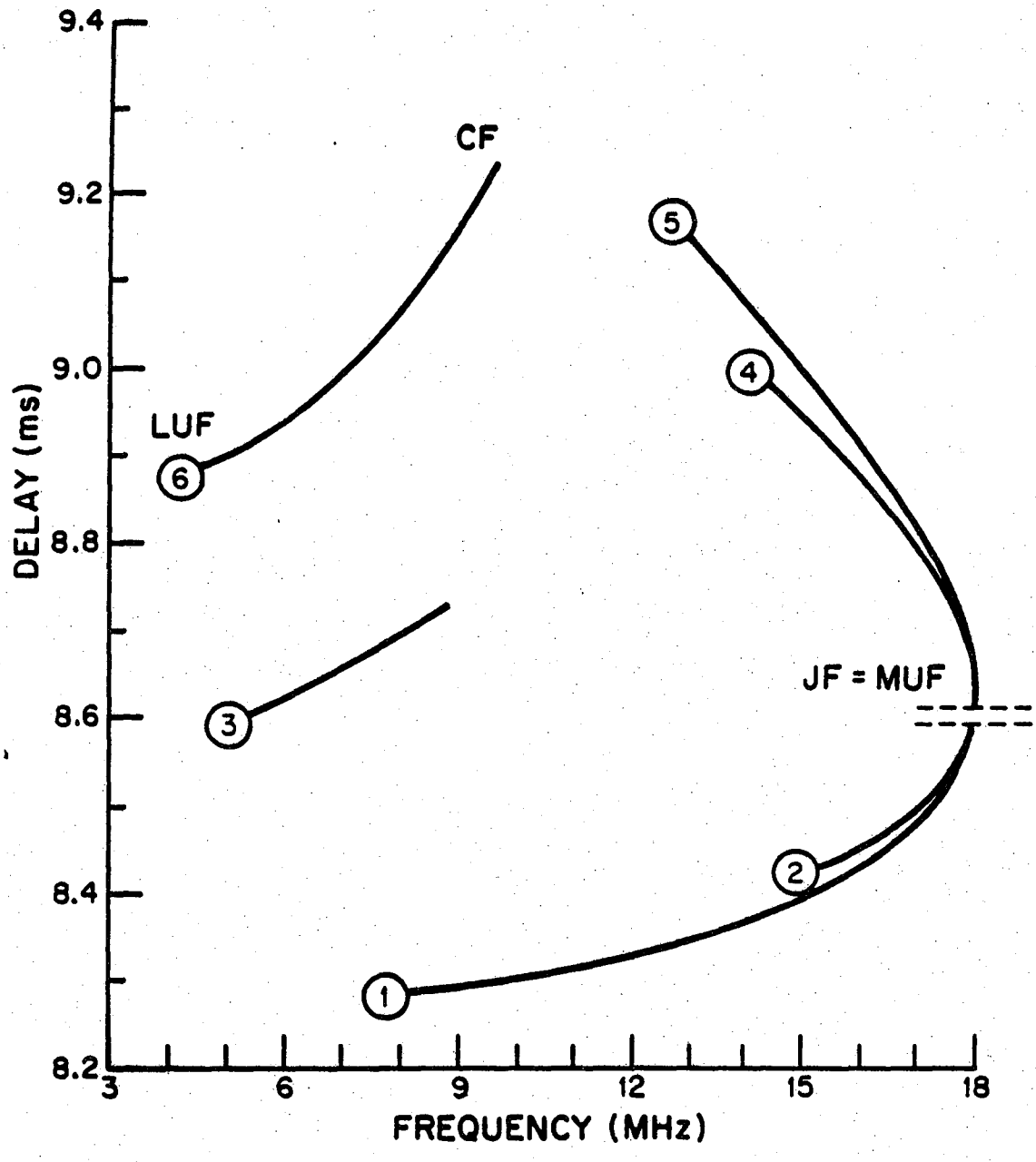

Figure 16. The six modes of an observed oblique incidence ionogram.

This WB model is claimed to be one possible generalization of the NB model described in (5) of Section 5.2. There may indeed be many other potential generalizations and extensions. However, to discern which candidate model is better and for what reasons would require experimental validation over real HF channels. Such programs are beyond the scope of this study.

The explanation of terms in the wideband H(f,t) of (6) is given next. Gradually, as needed, it is to be followed by justification arguments that support the assumptions made. The formal transfer function nomenclatures for both NB and WB models are briefly summarized in Table 9. There are more than a few similarities and differences to be stressed here.

First, the time-varying transfer functions for both are sums of all incident modes. An individual contributing mode is identified by index i. Its contribution to the transfer function is $H_i(f,t)$. So far, the two models obey the same additive and linear formalism. Returning to Figure 16 and its six modes, the sum would go from i=1 to i=6 and separate contributions to the transfer function would come from $H_1(f,t)$ to $H_6(f,t)$. Of course, individual modes can have a variety of properties at given frequencies. This is incorporated in the WB model, as it was done for NB, through specification of modal components, $H_i(f,t)$. See the second row of Table 9.

Next, the definition of all elements in $H_i(f,t)$:

$A_i(f)$ = Real, nonnegative, amplitude for the i-th mode at frequency f. It is a constant number with respect to time and can be zero for all those frequencies where the mode vanishes. This dependence on f is unnecessary and therefore absent in all former narrowband models. However, in wideband observations that led to Figure 16 and elsewhere, variations with f have been noted. In particular, mode 1 in Figure 16 shows a high amplitude peak just below the MUF. To complicate things further, between 10 and 17 MHz that same mode displays a noticeable oscillatory behavior as a function of f. In as much as this phenomenon persists both in the presence and absence of mode 2, plus an apparent periodicity of mode 2 itself, this effect may be due to magneto-ionic, or O and X, ray splitting and possible crossovers of the modes. If that were shown not to be the case, rationale should be developed either to incorporate this effect into the amplitude function, $A_i(f)$, or to ignore it as something of secondary importance.

$u_i(f,t)$ = Complex, bivariate Gaussian, random process in time t, with zero means and statistically mutually independent

Table 9. Formal Differences Between Narrow- and Wideband Models

Characteristic Description	Narrowband Model (NB)	Wideband Model (WB)	
1. Time-varying transfer function for the entire HF channel	$H(f,t) = \Sigma H_i(f,t)$		
2. Time-varying transfer function for an individual mode, $H_i(f,t)$	$C_i(t) \exp[-j2\pi\tau_i f]$	$A_i(f)\, u_i(f,t) \exp[-j2\pi\tau_i(f)f]$	
3. Time-varying multiplier factor(s) for an individual mode	$C_i(t)$	$A_i(f)$	
		$u_i(f,t)$	
4. Time delay characteristic for an individual mode	τ_i	$\tau_i(f)$	$\overline{\tau_i(f)}$
			$\tau_i(f) - \overline{\tau_i(f)}$

components. For every fixed frequency, f, this function is quite similar to the NB tap-gain multiplier $c_i(t)$, except that $u_i(f,t)$ is to have unity rms values for both quadrature processes. For the special narrowband case, the f-dependence can be neglected in both $u_i(f,t)$ and $A_i(f)$. Their product then is equivalent to the frequency insensitive $c_i(t)$. This correspondence is indicated in row 3 of Table 9. The WB Doppler spreads and shifts are generated by this $u_i(f,t)$-process. That includes the familiar spectral shaping from before, except that now the center frequencies and the spreads of the Doppler spectra can be varied across the arbitrarily wide channel bandwidths that are to be simulated. Just how large the bandwidth must be for the f-dependence to become significant is not at all well established. However, based on reported past work, that bandwidth should be at least 10 kHz--and perhaps much higher.

$\tau_i(f)$ - Frequency sensitive path delay encountered by the i-th mode. As illustrated in earlier ionograms (Figures 5, 6, 14, 15, and 16) the mode delay appears to be constant only over a relatively narrow band. Even for NB applications, some workers have deemed it necessary to include dispersion filters that in effect reproduce the same delay scatter (or spread) as would a delay entity with a linear delay-versus-frequency characteristic. For WB models, depending on the occupied spectral region, the first, second, and even higher order derivatives of $\tau_i(f)$ with respect to f may be of significance. For example, mode 1 in Figure 16 seems to resemble a parabola with a bothersome singular slope at one end. Since most of the transmitted channel energy may occur at that frequency, an issue about the importance of such nonlinearities arises. If their impact could be downgraded enough, perhaps piecewise linear approximations of the delay functions would be justified. The last line of Table 9 goes a step further. Let the TDL tap for the i-th mode be set at some representative (or average) value. Then the rest of the delay curve may be left up to specific system implementations.

A final comment on this hypothetical modeling approach deals with the issue of statistical dependence versus independence, or crosscorrelations versus absences thereof. Since all random elements of the WB communications channel somehow share the same common physical medium, i.e., the ionosphere, one can argue that some mutual statistical dependence must exist. But, whatever its constitution, that dependence appears either unknown or extremely complicated. To make some progress in a practical sense and to initiate a dialogue, one proposes the following Null Hypothesis:

For engineering purposes in hf channel modeling, and unless shown otherwise, all random variables and processes contained in the time-varying channel transfer function h(f,t) are mutually uncorrelated.

It could then be up to future experimenters and statistical analysts either to prove, disprove, or modify the above Null Hypothesis. Or, as before, it would remain the burden of the HF system designers and communicators to carry on without an answer to this question.

6.2 Required Experimental Data

Watterson's modeling of the narrowband HF channel in terms of its time-varying transfer function was discussed in Section 5.2. Experimental verification of said model was the topic of Section 5.4. Measured data established the validity of that model. Eventually, an NB simulation facility was implemented. It met the channel specifications listed in Table 4.

Unfortunately, despite many old and new reported experiments, no such happy state of affairs exists for the wideband HF channels (NBS, 1948; Koch et al., 1960; Nupen, 1960; Auterman, 1962; Davies, 1965; David et al., 1969; CNR, 1979; Haines and Weijers, 1985; Skaug, 1981, 1982, and 1984; Kashian et al., 1982; Wagner and Goldstein, 1982 and 1985; Perry, 1983b; Taylor and Shafi, 1983; Wagner et al., 1983; Reinisch et al., 1984; Sues and Haines, 1984; Salous, 1985; Malaga, 1985; Perl and Kagan, 1986). Although only one WB model has been emphasized here (see Equation (6) and Table 9 in Section 6.1), the root of the difficulty seems not to be associated with a shortage of models. Many WB models can be conjectured and analyzed ad infinitum. Instead, the root of the problem appears to be tied to a genuine shortage of knowledge about this medium. Let us return to the comparison of narrow- and wideband models in Table 9 and ask for facts and numbers about the wideband model. The answer is a disappointing one. Very little is known. The number of multipath modes can be deduced from ordinary ionograms. So can the delay characteristics, $\tau_i(f)$. The behavior of mode amplitudes as a function of frequency, $A_i(f)$, could be obtained with more sophisticated ionosondes. But, unfortunately, either they are not fully instrumented or the data are not processed. For delay dispersions, Doppler shifts and spreads, etc., even less is known. The existence of statistical properties and the fine structure of random multiplier functions $u_i(f,t)$ are indicated in recent Naval Research

Laboratory tests (Wagner and Goldstein, 1982 and 1985). However, useful and representative parametric value summaries remain undetermined for f bands that exceed 10 kHz or so. The bottom line is a simple conclusion that without further experimentation one has no way of ascertaining whether any proposed H(f,t) is or is not a valid model.

Assume for a moment that a virtual plethora of experimental facilities were suddenly made available for HF measurement programs. What types of data would one seek? A way to answer this question may be to return to Tables 4 through 9, and to ask what parametric changes are anticipated for broader ranges of frequency. The issue is addressed in Table 10.

Note that Table 10 has the same parameter field as its NB counterpart, i.e., Table 4. And, in fact, some parameters may agree further and retain the same or similar numerical sets in both versions. When that is the case, Table 10 displays a "Same as NB" entry in its second column. Examples are the number of modes (or paths), signal-to-noise ratio settings, atmospheric noise, man-made noise, or interference classifications, diversity order, and so on. Other parameters show different values and different behavior. One such parameter appears to be the bandwidth, which for WB systems must be in the range of megahertz. Typical bandwidth values suitable for spread spectrum systems are indicated in the top row of Table 10. Thereafter follow eight parameters that were constants for the NB model, but, to be safe, may have to be replaced by functions of f in the WB scenario.

The eight, potentially f-dependent, quantities are

1. Delay(s)

   As discussed, every propagation mode i in the channel bandwidth has its own delay-versus-frequency characteristic. One calls it $\tau_i(f)$. Seldom is this function a constant for bandwidths approaching 1 MHz. To simplify modeling, the function may be approximated by piecewise linear segments. It is hoped that one, two, or at most three linear segments will suffice in practice. For realistic HF paths, the absolute propagation delay is less than 10 ms. The differential delays between paths are usually on the order of 1 ms (see Figure 16).

2. Dispersion Slope

   For every mode, dispersion of energy in time contains a part proportional to the magnitude of the delay derivative with respect to f. While there may be other sources that contribute to the time

Table 10. Tentative WB_Simulator Specification

Parameter	Values
Bandwidth (MHz)	.2, .5, 1, 2, 3*
Modes or Paths (number)	Same as NB
Delay(s) (ms)	Function(s) of f
Dispersion Slope (μs/kHz)	Function(s) of f
Specular Atten. (dB)	Constant over f
Specular Phase (radians)	Constant over f
Scatter Atten. (dB)	Function(s) of f
Frequency Shift (Hz)	Function(s) of f
Frequency Spread (Hz)	Function(s) of f
Fading Spectrum (shape)	Function(s) of f
Signal to Noise (dB)	Same as NB
Atmos. Noise Vd. (dB/2.7 kHz)	Same as NB
Man-Made Noise (class)	Included*
Signal to Interfer. (dB)	Same as NB
Interference Type (CW, pulse, PB)	Same as NB*
Diversity Order (number)	Same as NB
Internal Distortion (dB vs S+I+N)	Same as NB

DETAIL

Piecewise linear $\tau_l(f)$ [less than 10 ms]
Step function $\lvert\dot{\tau}_l(f)\rvert$, plus piecewise linear other scatter [sum less than .2 ms/MHz]
Only for a single specular component
Only for a single specular component
Piecewise linear $A_l(f)$, where nonzero
Linear (mean) Doppler shift due to $u_l(f,t)$
Linear Doppler spread due to $u_l(f,t)$
Two Gaussian functions that as a function of f can merge and become one Gaussian function

*To be further specified

delay scatter in the modes, the point is that distinctly unique dispersion functions may be required by individual modes. For simplicity, step functions or piecewise linear approximations may suffice. Per multipath mode, the dispersion slope may have to be bounded by a value yet to be determined.

3. Specular Attenuation.

In the more common situations, either none or at most one specular wavefront is received. Then the assumption of a constant specular attenuation over all f appears justified. However, if there are two or more specular components, even relatively mild phase fluctuations can cause nulls and peaks at sufficiently separated frequencies.

4. Specular Phase

If there is one specular term, its phase could be treated as a constant. However, in the infrequent case of more than one specular term, special adjustments--such as uniformly distributed phase differences--may be appropriate in the WB model.

5. Scatter Attenuation

Each received multipath mode shows some amplitude dependence on frequency f. The function has been denoted as $A_i(f)$ for the i-th path. When attenuation is total at a given f, no energy is received, and the function vanishes. For ease of representation, a small number of piecewise linear segments may suffice to approximate the scatter attenuation function of a mode.

6. Frequency Shift

As a function of f, the average Doppler shift of a mode i may differ from other modes. This functional dependence on index i and on frequency f must be incorporated in the complex, bivariate Gaussian, random tap multiplier function $u_i(f,t)$ of equation (6). A single linear function over f appears the easiest model for the Doppler shift. The magnitude of the Doppler shift should typically remain below 10 Hz.

7. Frequency Spread

This is the rms value of the modal Doppler spread. Just like the Doppler shift, its functional behavior is part of the random multiplier function $u_i(f,t)$. Again a single linear function over f should suffice for each multipath mode. The frequency spreads are normally on the order of 1 Hz.

8. **Fading Spectrum**

The spectral shape of $u_i(f,t)$ has only one peak when there is no magneto-ionic path splitting. When splitting occurs, each of the O and X components has its own peak. In all cases, the shapes are to be Gaussian functions with relative displacements that vary linearly with frequency.

It has been stressed repeatedly that the objective of wideband HF measurements need not be to record every detail of the proposed channel model, and certainly not the complete frequency dependent characteristics of H(f,t). There are two reasons for that. First, due to the great variability of the HF channel, the entirety of traits would be incredibly difficult to establish with any degree of confidence. Second, details that are too complex may be impossible to model and to simulate with the state-of-the-art technology. It appears far more expedient to seek channel representations based on simple approximations. That is the motivation for utilizing piecewise linear segments to fit only a few selected functions of frequency, such as $A_i(f)$, $\tau_i(f)$, and so forth. Furthermore, the number of segments is to be kept low, say at one, two, or three.

As examples of such approximations consider Figures 17 through 19. All three show a channel with a 3-MHz bandwidth. That bandwidth, however, is not positioned in the same location of the HF spectrum. Figure 17 occupies 3 to 6 MHz, Figure 18 from 9 to 12 MHz, and Figure 19 from 16 to 19 MHz. All are plotted to illustrate the diverse nature of the same HF medium, at the same time, over the same radio path. In fact, the multipath structure underlying them all is that of Figure 16. Various portions of the six modes, which are shown to occupy the region between the LUF (4 MHz) and the MUF (18 MHz), occur in the composite picture.

Since the LUF falls in the middle of the band in Figure 17, only half of the 3-MHz bandwidth will support any signal. The signal received is carried on two modes (for notation see Figure 16), numbered as 6 and 3. Mode 6 contributes from 4.5 to 6 MHz. Mode 3 contributes from 5.2 to 6 MHz. Five properties of the two modes are plotted in separate subfigures. They are mode delays, dispersions, attenuations (amplitudes), frequency shifts, and frequency spreads. All are approximated with at most two straight-line segments. Note that the mode delays in the uppermost plots correspond directly to the ionogram (Figure 16). The ionogram also provides at least partial input

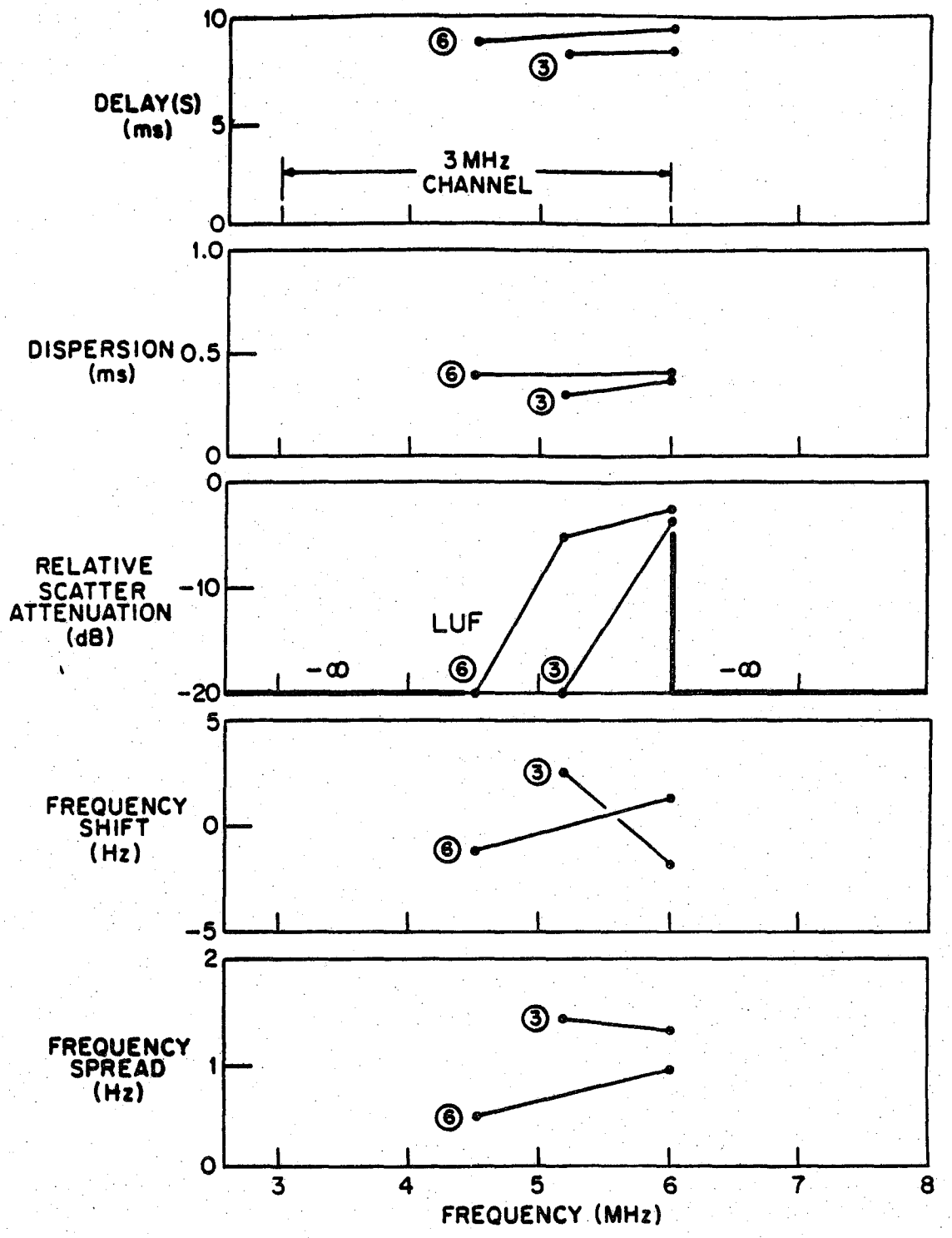

Figure 17. Example of function modeling in a 3- to 6-MHz band.

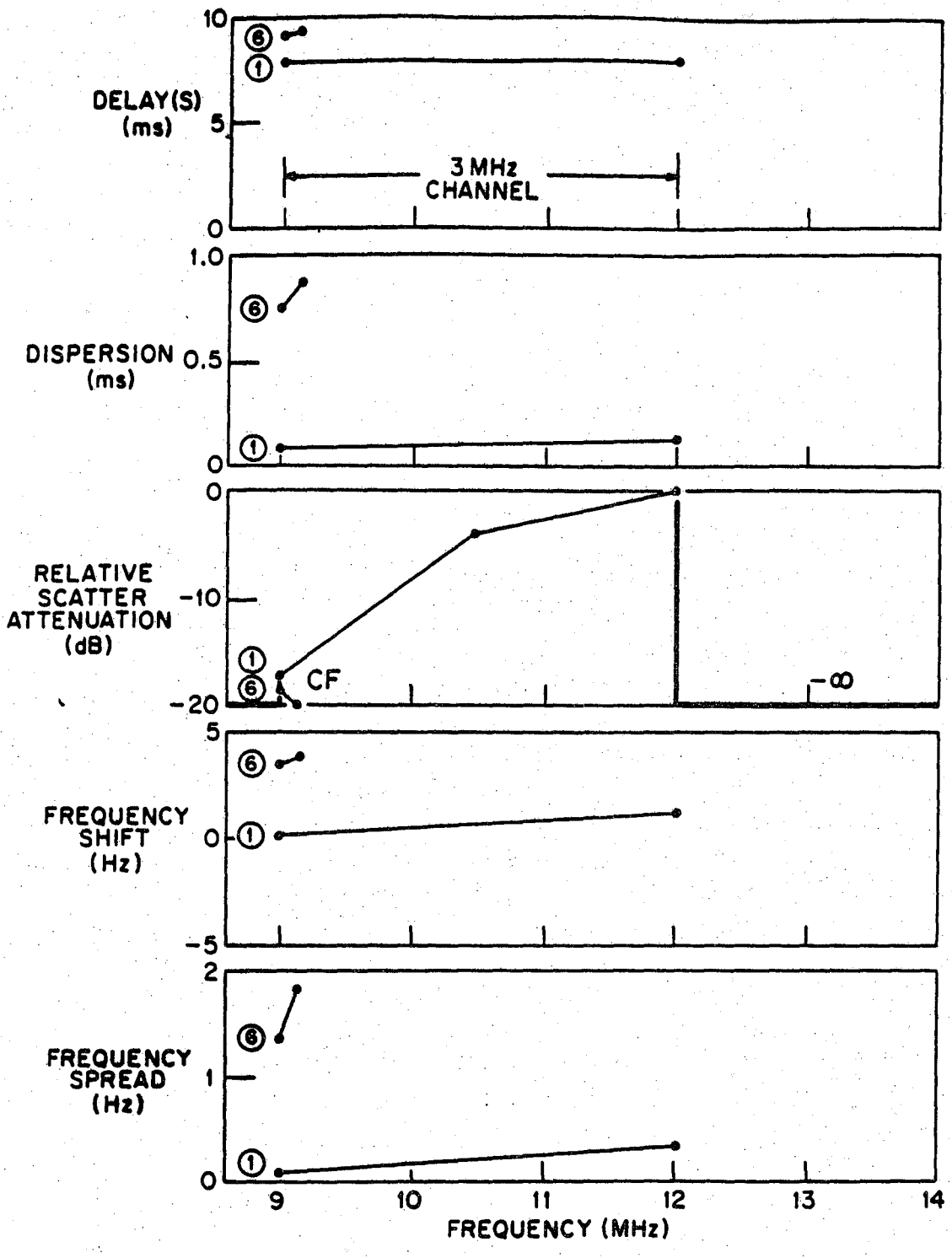

Figure 18. Example of function modeling in a 9- to 12-MHz band.

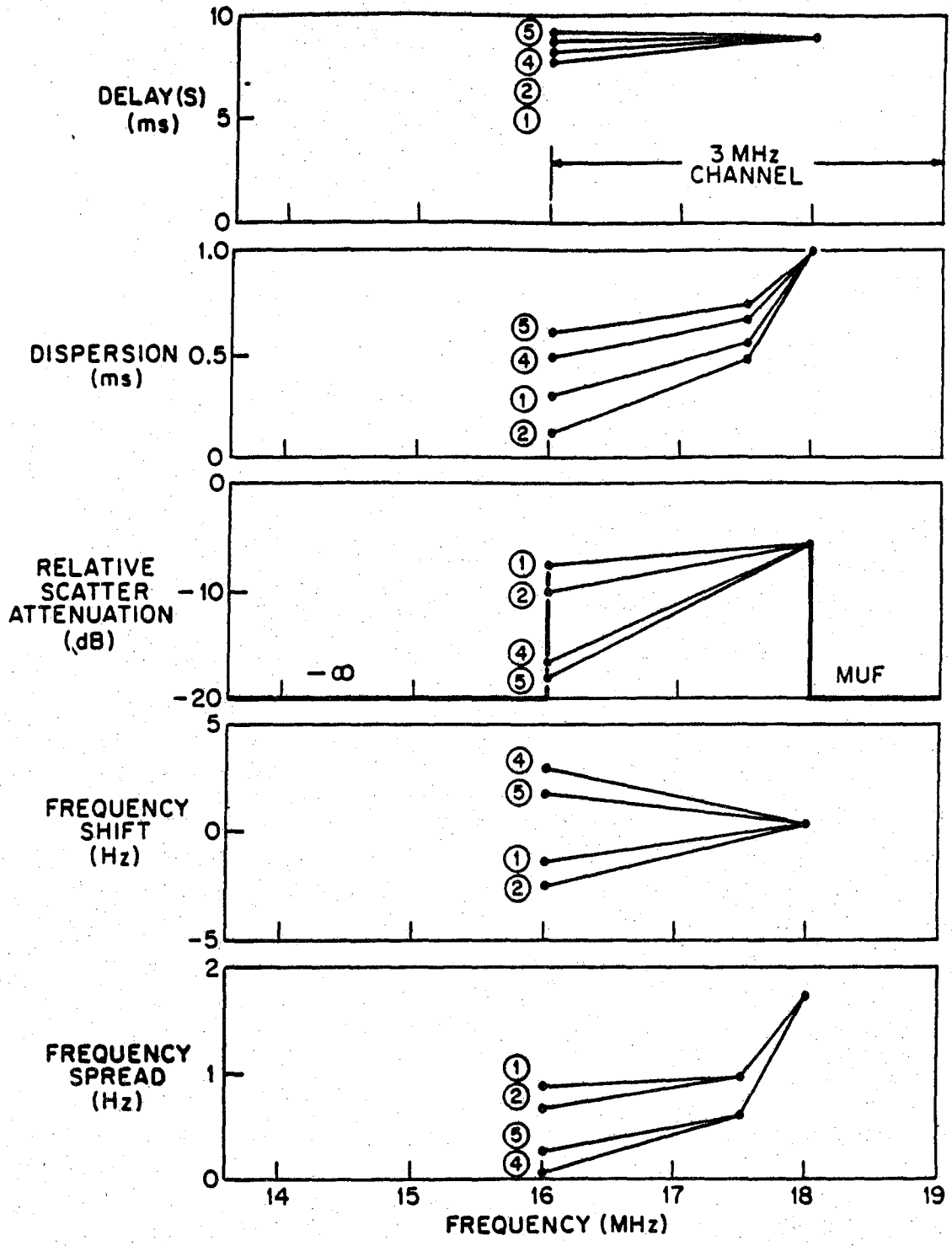

Figure 19. Example of function modeling in a 16- to 19-MHz band.

for dispersion plots in the second subgraph from the top. However, as it is shown, the ionogram of Figure 16 offers no dB numbers to the relative attenuation profiles in the third subgraph. Additional ionosonde enhancements are needed for estimation and recording of component amplitudes. The lowest two graphs, namely frequency shift and frequency spread, are not derivable from Figure 16. In fact, for any WB channel of interest, woefully little is known about their actual behavior. The straight lines in Figure 17 are entirely conjectural and included to illustrate the principle.

Figure 18 shows the signal is received over the entire 3-MHz bandwidth. For most of the band, apparently, there is only one mode present. That is mode 1 of Figure 16. In the typical HF language, one could say that there is essentially no multipath in this channel. Of course, between 9 and 9.2 MHz, one gets a glimpse of mode 6. At that frequency the difference between mode delays may be the largest in the ionogram and the particular frequency would be defined as the CF. However, the energy of this spectral skirt appears quite depressed. Eventual simulation runs could confirm irrefutably whether for certain systems the distortions due to mode 6 are or are not negligible.

The 3-MHz bandwidth window in Figure 19 is unique in the sense that it contains four multipath modes. In Figure 16 they were originally numbered as 1, 2, 4, and 5. These modes converge at the Junction Frequency (or the 18-MHz MUF in this instance). There is no significant radio-wave reception observed above the MUF; however, the more interesting questions pertain to the behavior of delay dispersion and Doppler effects near the MUF. Is it really justified to bound the above functions of frequency, as was done in Figure 19, when the true ionogram (Figure 16) implies a slope of infinity? Otherwise, the piecewise approximation with a few straight-line segments is used in this Figure 19 as it was done in the previous ones.

In a summary for this section, experimental data are needed for wideband HF modeling:

- to validate the overall model, H(f,t), of (6)
- to identify the most significant functional elements of H(f,t)
- to establish typical and extreme quantitative ranges for the significant functional elements of H(f,t)

- to justify simple approximations for the significant functional elements of H(f,t)

- to test the Null Hypothesis of mutual statistical independence and lack of correlation between random components of the significant functional elements of H(f,t)

- to find the duration of time intervals during which these random components can be considered stationary

6.3 Spread Spectrum Considerations

The previous Section 3 on HF spread spectrum (SS) radio technology describes five general types of systems. They are

- Direct Sequence (DS)
- Frequency Hopping (FH)
- Time Hopping
- Linear Frequency Modulation or Chirp
- Hybrid Systems (DS/FH)

The DS, FH, and the hybrid systems are of most interest to this study. For additional background on spread spectrum systems and their HF applications, see Gerhardt and Dixon (1977); Thrower (1978); Milstein et al., (1980); Pursley (1981); Milsom and Slator (1982); Low and Waldstein (1982); Holmes (1982); Chow et al., (1982); Cook et al., (1982); Cook and Marsh (1983); Mahmood (1983); Dixon (1984); Geraniotis and Pursley (1985 and 1986); Simon et al., (1985); Skaug (1985); Bird and Felstead (1986); and Siess and Weber (1986).

The DS and FH/DS systems spread their energy or power density more or less continuously, to the exclusion of persistent spectral null zones in the bandwidth of concern. As such, they involve the entire channel at all times. In modeling and simulation of DS and FH/DS systems, one therefore appears to require the full bandwidth of the wideband channel. No easy modeling shortcuts are readily apparent here.

However, some simplifications may be possible for the pure FH systems. The typical frequency hopper periodically hops from one frequency, f_i, to another. While transmitting at each frequency f_i, the instantaneous signal bandwidth may be somewhere between 3 and 12 kHz. At that time its spectrum appears as narrowband. If the whole set of FH frequencies consists of

M frequencies, such as f_1, f_2, f_3, . . ., f_M, then a conceptual parallel bank of M narrowband channel models could suffice. Figure 20 shows how a wideband filter is decomposed into a summation of adjacent narrowband filters. Thus, within the band of interest,

$$F(f) = F_1(f) + F_2(f) + \ldots + F_M(f).$$

Raised-cosine or other ripple reducing filters may be used for the NB elements.

Some problems still remain for this FH model. Perhaps the most significant question pertains to the mutual dependence (or independence) and crosscorrelation between the M narrowband models. Let us assume that M narrowband, Watterson type, NB simulators are implemented. According to the hopping regime, the signal occupies one filter (i.e., simulator) at a time. In each filter, the channel transfer function parameters assume their respective values. That includes the number of paths, their time delays, amplitudes, dispersions, and all the other variables specified in Table 4. But how are these related to each other and in different bands? More data are needed, especially for those bands that are adjacent to each other. Since a common value for the number M may easily be in the hundreds, the specification of the M-times-M dependence supermatrix is by no means trivial. Unless, of course, one is prepared to accept the independence or Null Hypothesis postulated at the conclusion of Section 6.1. One should also add that a parallel implementation of M=100 NB machines is likely to be unrealistic. Some sequential, very high speed, technology is more promising for this approach.

6.4 Potential AI Enhancements

Artificial Intelligence (AI) is a relatively recent field. It has a programming background that depends heavily on powerful computer resources. In the last several years it has developed new specialized subareas, such as expert systems, rule-based systems, knowledge base systems, and related inference engines, that individually or jointly may be useful to automate HF channel modeling.

Within this work, neither the nature nor applications of AI has been studied in depth. However, that does not imply that planning of HF experiments, their interpretation, analysis, model synthesis, and perhaps eventual simulator implementation, could not benefit from AI now or in the

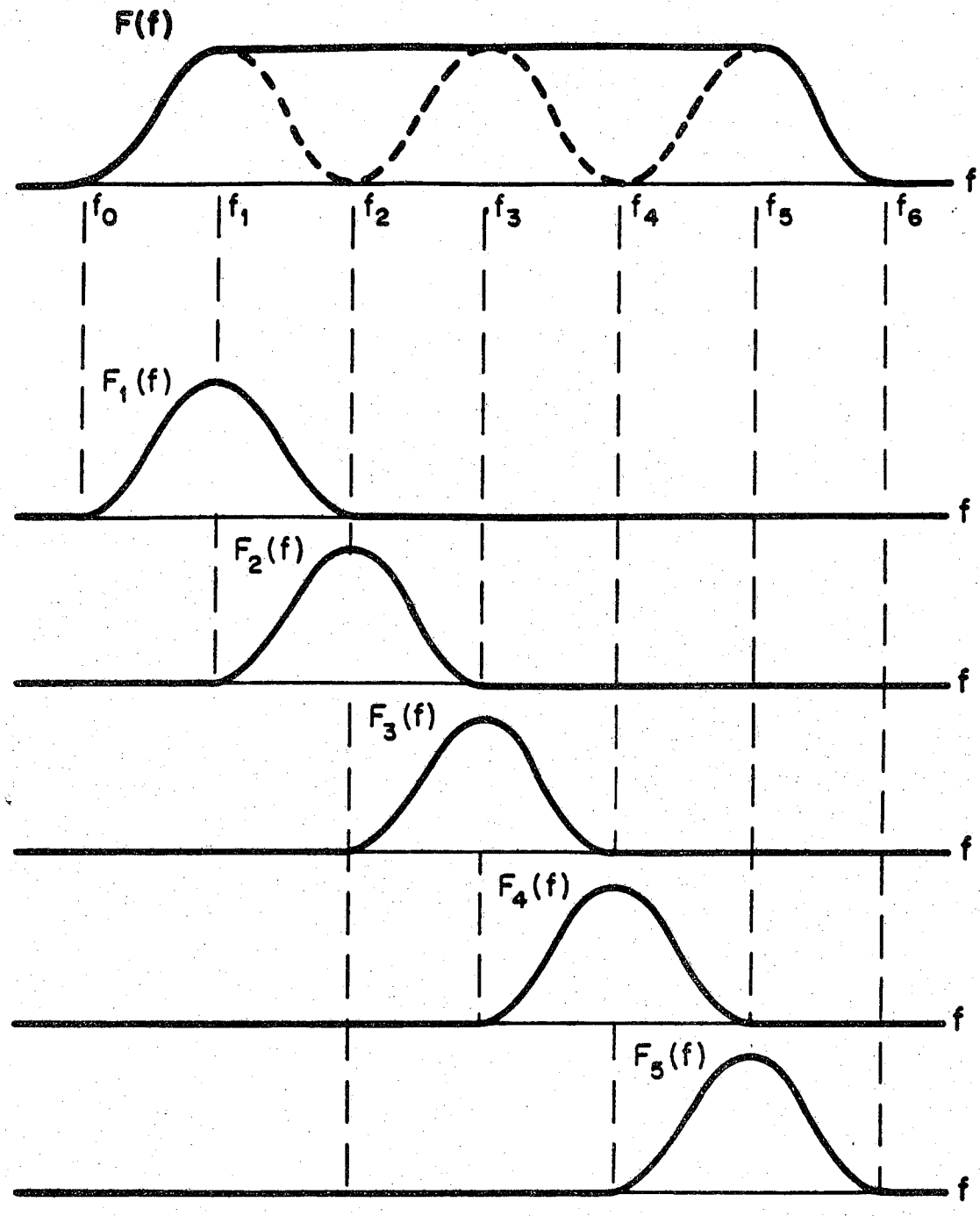

Figure 20. Decomposition of a wideband filter into a sum of narrowband filters.

foreseeable future. At this time it should suffice to give a few definitions and motivational comments.

As applied to HF, a knowledge base would be an automated data base that contains factual information about pertinent physics, ionospheric properties, radio-wave propagation, device characteristics, observed statistics, mathematical equations, algorithms, rules, facts, and assorted conditional information. The knowledge base, combined with guesses, rules of thumb, and heuristics, would be one input to the knowledge base system. The other input would come from sensory drivers, which in the HF case would be received signal waveforms and supporting measurements. The output of the knowledge base system is to be inferences about the HF channel model. Examples of inference could be to propose new channel H(f,t) models, or to validate an already proposed model, to diagnose strange behavior, or to prove or disprove any of the allegations raised in Sections 6.1 and 6.2.

To generate the required knowledge, an expert may have to be utilized. This expert could be one or several individuals, recognized for their exceptional mastery of the HF communications field. Anything they know about HF could be summarized and submitted to the system. The actual interface between the expert and the system, also called the expert system may end up in the hands of another individual, the knowledge engineer. There must be correct procedures, logic, and rules that govern the processes of the systems, especially when they perform computational and analytical tasks. Systems whose rules are structured along the lines of condition-action or simple if-then steps, are called the rule-based systems.

Which combination of the above has the best promise for HF modeling is not at all clear. However, the AI field seems to be advancing with such an amazing pace and its applications are expanding, that it leads one to believe that the question will answer itself in the near future.

7. WIDEBAND HF CHANNEL SIMULATORS

Previous workers have described the advantages of channel simulators for evaluating radio performance (CCIR, 1974; Watterson and Minister, 1975; Watterson, 1979 and 1981; Hoffmeyer et al., 1984). The advantages include repeatability, availability, a broad range of channel conditions, completeness, accuracy, and lower cost. These general advantages apply for a wide variety of

channel simulators: HF, troposcatter, and line-of-sight (LOS) microwave. However, these advantages are debatable when the model on which the simulator design is based is in doubt. Ultimately a reliable model must be based on empirical data rather than on conjectures or mathematical axioms. A validated model based on HF channel measurements exists for narrowband HF sky-wave channels. An equivalent validated model does not exist for wideband channels, however.

Table 11 lists the types of signal distortions that occur on HF sky-wave channels. Models for each of these types of signal distortions are well understood and can be simulated for narrowband channels. This is not true for wideband HF sky-wave channels. In particular, wideband models are needed for dispersion (which is negligible for narrowband channels), noise, and interference.

There are several ongoing efforts to develop a wideband HF channel simulator. Much of this work is an attempt to extend the Watterson/CCIR model concept. This work is described in the following paragraphs. Emphasis is placed on the identification of potential limitations of these wideband simulators. None of these simulators are based on a general wideband channel model that has been verified through sufficient wideband propagation measurements.

Table 11. Types of Signal Distortion in HF Sky-Wave Channels

General Types of Channel Distortion		Specific Types of Channel Distortion
Additive	Noise	Thermal noise Impulsive noise
	Interference	Unwanted signals
Multiplicative	Time scatter	Multipath differential delay dispersion
	Frequency scatter	Multipath differential Doppler

7.1 Signatron Wideband Channel Simulator

Ehrman (1984) reports on modifications of the Signatron simulator for "wideband" application. This simulator, whose principles were described earlier in Section 5.3, has been extended to a 12-kHz bandwidth, and has been modified for following a frequency-hopping modem. The basic channel still follows the Watterson model. The paper by Ehrman does not describe how the Watterson model was modified for frequency-hopping operations. The significance of this question can be seen from an examination of Figure 21. The figure depicts a time/frequency pattern representative of a frequency-hopping HF system. Questions related to the correlation interval in both the frequency and time domains are apparent. If the time interval between dwells on a given frequency is large enough, the channel parameters can be considered to be statistically independent. But, what is this time interval, and what is the correlation as a function of time? Does it depend on the frequency band? Analogous questions apply in the frequency domain. What is the frequency decorrelation interval? The resolution of these issues in the "wideband" Signatron model/simulator is not clear from Ehrman's paper.

The "wideband" version of the Signatron simulator cannot be easily extended to bandwidths approaching 1-MHz because the processing requirements would be much too high for the Floating Point Systems array processor.

Several Government organizations utilize the Signatron wideband simulator including the Naval Research Laboratory in Washington, DC, and the U.S. Army Center for Communications (CENCOMS) at Ft. Monmouth, NJ.

7.2 NOSC Wideband Channel Simulator

The Naval Ocean Systems Center (NOSC) has conducted research in the area of wideband (96-kHz) measurements, modeling, and simulation (Hoff and King, 1981). They extended the Watterson model by including a delay distortion filter in their simulator, as seen in Figure 22. As noted earlier, this is necessary because wideband signals propagated via the ionosphere become distorted due to dispersion. This can be seen from the ionograms previously given in Figures 5, 6, and 16. If the propagation delays versus frequency were horizontal lines, all frequencies would be delayed the same. Each delayed signal in an individual mode would be undistorted provided the path loss were constant across the frequency band. However, the ionograms are not constant

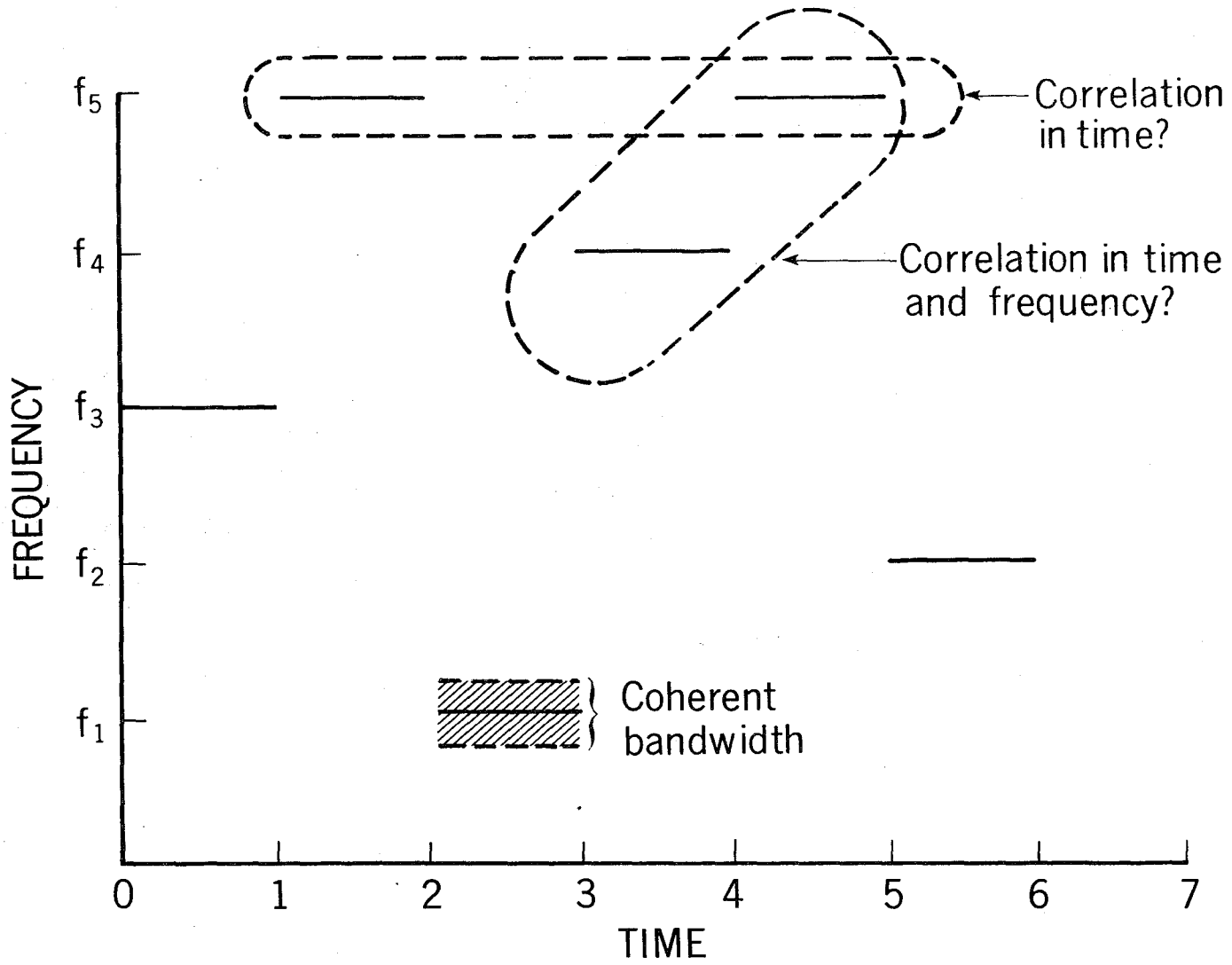

Figure 21. Wideband frequency and time correlation interval modeling for testing FH sky-wave radio.

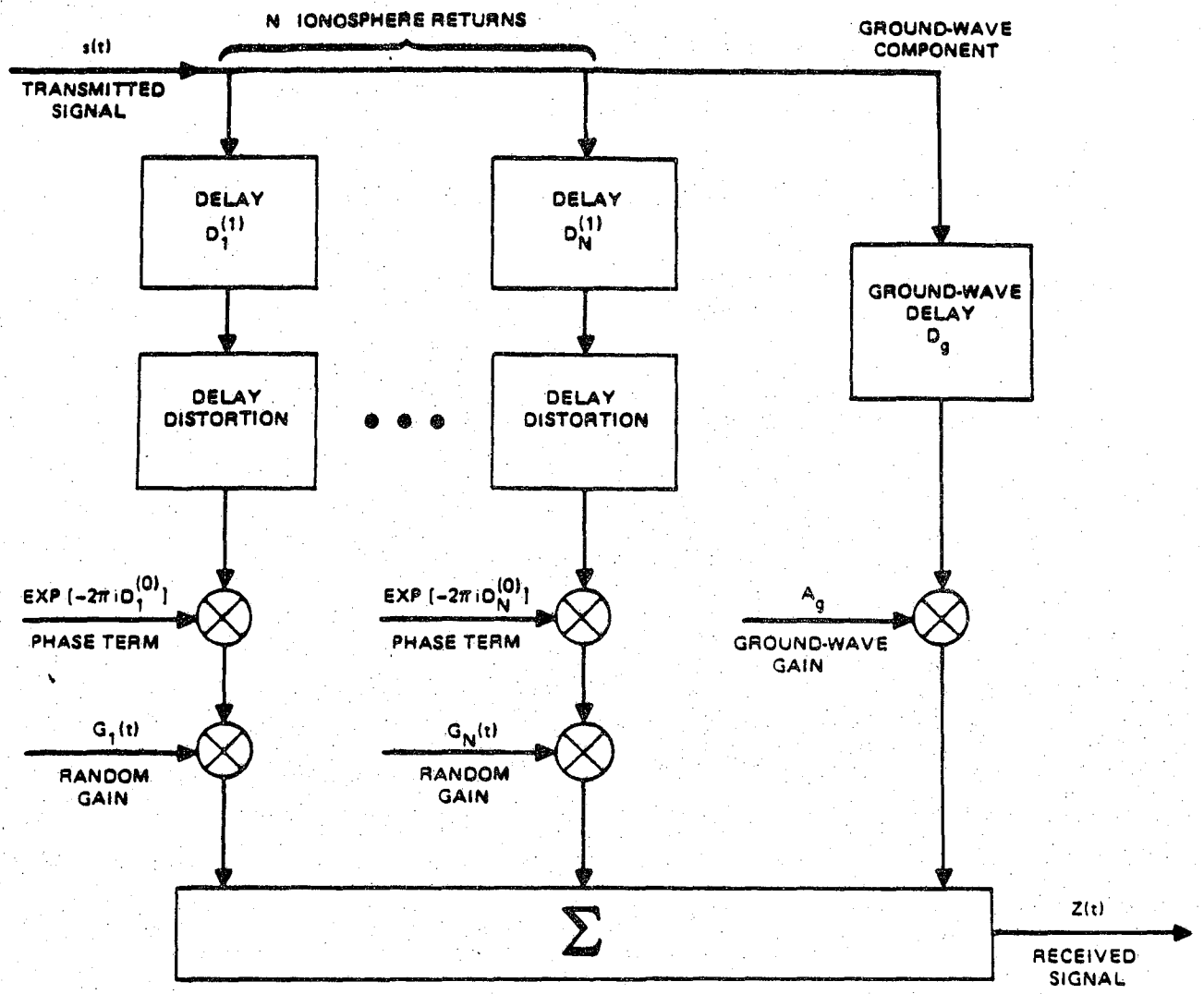

Figure 22. Block diagram of the NOSC wideband HF channel simulator.

horizontal lines and the path loss is, in general, nonuniform with frequency. Thus, a distortion filter is required for simulating wideband channels. This is the main difference between the Watterson/CCIR narrowband model and the NOSC wideband model.

Hoff and King (1981) describe an experimental program for collecting wideband (96-kHz) propagation data on a 232-km sky-wave path. The purpose of this measurement program was to collect data to verify the NOSC wideband channel model. The analysis of these data has not been reported.

The NOSC wideband model was implemented in a computer program that runs on a general purpose computer. This implementation is not designed for real-time performance evaluation of wideband HF modems. It has been used for the evaluation of adaptive equalizers simulated in software.

7.3 MITRE Wideband Channel Simulator

The MITRE Corporation has initiated the development of a wideband (1-MHz) HF channel simulator (private conversations with Mr. B. Perry, MITRE Corp.; Bedford, MA; and Mr. J. Barratt MITRE Corp., McClean, VA). This recent program has not been described in any existing reports and, therefore, will be briefly described here.

The MITRE wideband simulator utilizes high-speed signal processing integrated circuit chips developed by MITRE. The simulator incorporates a dispersive filter to simulate the group delay dispersion that must be simulated for wideband sky-wave channels. The range of dispersion is claimed to be from 0 to 100 μs/MHz. Taps on the dispersive filter are to be varied in real time. The model for controlling the dispersion is being developed. Additional wideband measurements for the validation of this model are desirable (private conversation with Mr. Perry and Mr. Barratt).

The MITRE simulator will be capable of evaluating the performance of either direct sequence or frequency-hopping HF radios. The hop range of the latter would be restricted to a 1-MHz range. At this time, only a single channel is being constructed. Realistic simulation of the sky-wave channel will require at least four channels to be built (two major modes with the ordinary and extraordinary components for each mode).

8. SUMMARY AND CONCLUSIONS

A survey of wideband HF radio technology and wideband HF channel modeling plus simulation has been conducted. The survey consisted of both a literature search and contacts with numerous individuals working in the wideband HF arena. The literature search included an automated search of data bases that contain both classified and unclassified entries. The personal contacts included people both in Government and in industry.

The purpose of investigating wideband HF radio technology was to develop general requirements for a future wideband HF channel simulator. Key questions are related to the expected bandwidth of direct sequence sky-wave radios and to the expected frequency hop rate of both sky-wave and surface-wave radios. Because spread spectrum HF technology is still in its infancy, the subject was treated more from a futuristic point of view than from the point of view of what is available today. Thus, numerical characteristics of specific radios were not provided. Instead, spread spectrum radio technology was treated in Section 3.2 from a feasibility viewpoint, given the constraints imposed by both the HF propagation channel, as well as the present state of hardware technology.

Table 12 summarizes the limitations of spread spectrum radio technology that were discussed in Section 3. It is concluded that a wideband HF channel simulator should be capable of testing direct-sequence radios having a bandwidth as high as 1 MHz, and frequency-hopping radios having a hop rate on the order of 10,000 hops per second. There is a fair amount of controversy about the allegations that radios, having these characteristics, are or are not practical due to ionospheric propagation constraints. Nevertheless, it appears desirable to have a channel simulator available to test the performance of prototype systems having these extended characteristics. Such testing could be performed over a full range of expected channel conditions, not just a limited set of conditions encountered during a typically short field test program.

As discussed in Section 3, an important technical issue concerns the coherent bandwidth of HF sky-wave channels. Direct-sequence radios depend upon the coherent processing of received signals. Adaptive equalizers are needed to compensate for channel distortions due to intramodal multipath and dispersion. Although MITRE has developed a 1-MHz adaptive equalizer, it has not been tested under a wide variety of channel conditions.

Table 12. Summary of Spread Spectrum HF Radio Limitations

Propagation Mode	Frequency Hopping Systems	Direct-Sequence Systems
Sky wave	Hops limited by ionospheric constraints to the order of 100 hops/second.	Questions remain about the feasibility of systems beyond 100 kHz bandwidth. Some HF systems with a 1-MHz bandwidth may be possible for certain applications.
Surface wave	On the order of 10,000 hops/second may be feasible based upon hardware constraints. This could be affected by unwanted sky wave returns.	Primary question is the practicality and cost of the hardware needed to implement a wideband direct-sequence system.

Because of the ongoing technical debate about the practicality of a 1-MHz radio for sky-wave applications, we recognize that a 1-MHz sky-wave channel simulator is quite desirable. It would help resolve radio design and technical performance issues. Such a simulator is currently in the preliminary development stage at the MITRE Corporation.

Table 13 lists the current wideband simulators either available or under development. Only the MITRE development effort comes close to meeting the objectives for a wideband HF channel simulator to be used in evaluating the performance of future spread spectrum radios. One limitation of the future MITRE simulator is that it currently operates at baseband rather than at rf. We maintain that, when testing radio systems, it is often required to test the entire system. Therefore a wideband channel simulator that operates at rf should remain the ultimate objective for future programs. MITRE plans to develop a frequency translator that will permit testing at rf.

The two other simulators listed in Table 13 cannot meet the objectives of testing systems with signal bandwidths of 1-MHz. Furthermore, the NOSC simulator is designed for evaluating software-simulated adaptive equalizers. While this is extremely useful in the early design phase of a development

program, it is not a tool to be used in the evaluation of the actual transmitter/receiver hardware.

There is only one dominant final conclusion for this study. That is to recognize the need for pertinent measured data from the HF channel as a wideband (on the order of 1 MHz) channel. To help in the spread spectrum system development, the requirement for wideband HF simulators has been noted. However, every simulator is based on a model--call it mathematical, statistical, stored database, state driven, or an engineering approximation. That model must be a valid, experimentally verified, representation of the real medium. For HF, the only sufficiently verified models known to the authors pertain to narrowband channels. These are channels with bandwidths on the order of, or less than, 10 kHz. For larger bandwidths, such as 100 kHz or higher, there apparently is no corresponding validated model.

Table 13. Summary of Current Wideband HF Channel Simulators

Simulator	Bandwidth	Comments
MITRE	1 MHz	Single channel is in the development stage. Simulator will operate at baseband. Additional measurements are needed to verify the channel model for the dispersive filter, noise, and interference effects.
Signatron	12 kHz	Because of the limited bandwidth, this simulator cannot be used for evaluating direct-sequence radios.
NOSC	96 kHz	Implemented in software on a general-purpose computer. Cannot be used to evaluate HF hardware. Application is for the evaluation of software simulation of adaptive equalizers.

One should question how and why such a state of affairs could exist. After all, HF communications have existed for most of this century. Thousands of HF circuits, analog and digital, crisscross the globe every hour. Past reports on experimental and theoretical research abound. References to more than one thousand studies had been collected before 1960 (Nupen, 1960). There may be a combination of reasons. First, nearly all working circuits at HF are quite narrowband. They occupy no more than the standard 3-kHz voiceband, and usually less. Second, the strategy to combat HF misbehavior has been to rely on human operator skills. Predictions and frequency switching options are in the hands of operators. Third, a large percentage of the HF propagation tests have been devised, performed, and analyzed by individuals whose main intent has been and still is to understand ionospheric physics. Fourth, the HF channel is by and large unpredictable, randomly time-varying, with sudden variations from time to time, as well as from place to place. Its complex, nonstationary nature only becomes more so as one looks at wider bandwidths. Comprehensive measurement programs are necessary to remedy this shortcoming. The programs would have to employ sufficiently high resolution channel probes to measure in detail the HF channel responses over the required large bandwidths. The detail is to include identification and estimation of transfer function characteristics for all multipath modes that are present.

To be more specific and constructive, consider the wideband time-varying channel transfer function, H(f,t), proposed in Section 6.1 (see also Table 10 and the accompanying definitions of terms). That function, given earlier as Equation (6), is

$$H(f,t) = \Sigma_i \, A_i(f) \, u_i(f,t) \, \exp[-j2\pi\tau_i(f)f].$$

This model agrees with the convincingly validated Watterson model for narrowband channels. Unfortunately, without adequate verification via wideband HF measurements, the above H(f,t)--like many other possible conjectures--will represent little more than a hypothesis.

9. REFERENCES

Adams, R.T., and M.S. Klein (1967), Simulation of time-varying propagation by computer control, Conf. Record of ICC'67, p. 74.

Agy, V., K. Davies, and R. Salaman (1959), An atlas of oblique-incidence ionograms, NBS Technical Note 31, National Bureau of Standards (Boulder, CO).

Aprille, T.J. (1983), Filtering and equalization for digital transmission, IEEE Commun. Mag. 21, March, pp. 17-24.

Auterman, J.L. (1962), Fading correlation bandwidth and short-term frequency stability measurements on a high-frequency transauroral path, NBS Technical Note 165, National Bureau of Standards (Boulder, CO).

Balser, M., and W.B. Smith (1962), Some statistical properties of pulsed oblique HF ionospheric transmissions, Radio Sci. 66D, pp. 721-730.

Belfiore, C.A., and J.H. Park (1979), Decision feedback equalization, Proc. IEEE 67, pp. 1143-1156.

Bello, P.A. (1963), Characterization of randomly time-variant linear channels, IEEE Trans. Commun. Systems COM-11, pp. 360-395.

Belnap, D.J., R.D. Haggarty, and B.D. Perry (1968), Adaptive signal processing for ionospheric distortion correction, MITRE Technical Report MTR-746 (MITRE Corp., Bedford, MA).

Bird, J.S., and E.B. Felstead (1986), Antijam performance of fast frequency-hopped M-ary NCFSK--An overview, IEEE J. Sel. Areas in Commun. SAC-3, pp. 216-233.

Bolton, E. (1971), Simulating atmospheric radio noise from low frequency through high frequency, Rev. of Scientific Instr. 42, pp. 574-577.

Bowhill, S.A. (1981), URSI Review of Radio Science 1978-1980 (International Union of Radio Science, Brussels, Belgium).

Bowhill, S.A. (1984), URSI Review of Radio Science 1981-1983 (International Union of Radio Science, Brussels, Belgium).

Bussgang, J., B. Goldberg, and E. Getchell (1974), Simulation and probing of radio channels, Telecommun., January, pp. 20-24.

CCIR (1974), HF ionospheric channel simulators, Rept. 549, XIIIth Plenary Assembly, Volume III, pp 66-72 (ITU, Geneva, Switzerland).

CCIR (1982a), Recommendations and Reports of the CCIR, volume III: Fixed Services at Frequencies below about 30 MHz. Includes Report 357-1, Operational ionospheric-sounding systems at oblique incidence, pp. 65-68; Report 549-1, HF ionospheric channel simulators, pp. 55-61; and others (ITU, Geneva, Switzerland).

CCIR (1982b), Recommendations and Reports of the CCIR, volume VI: Propagation in ionized media. Includes Report 258-4, Man-made radio noise, pp. 177-183; Report 342-4, Radio noise within and above the ionosphere, pp. 184-196 (ITU, Geneva, Switzerland).

CCIR (1982c), Recommendations and Reports of the CCIR, volume I: Spectrum utilization and monitoring. Includes Report 670, Worldwide minimum external noise levels, 0.1 H_Z to 100 GH_Z, pp. 224-229 (ITU, Geneva, Switzerland).

CCIR (1983), Characteristics and applications of atmospheric radio noise data, Report 322-2 (ITU, Geneva, Switzerland).

Chang, N.J.F., J.W. Ames, and G. Smith (1980), An adaptive automatic HF radio, SRI International Report DNA 5570F for the Defense Nuclear Agency (DNA, Washington, DC).

Chase, D. (1976), Digital signal design concepts for a time-varying Rician channel, IEEE Trans. Commun. COM-24, pp. 164-172.

Chow, S., J.K. Cavers, and P.F. Lee (1982), A spread spectrum modem for reliable data transmission in the high frequency band, Second Conf. on Commun. Systems and Techniques (London, UK). [Also available as IEE Publication No. 206, pp. 125-130.]

Claasen, T.A.C.M., and W.F.G. Mecklenbrauker (1985), Adaptive techniques for signal processing in communications, IEEE Commun. Mag. 23, November, pp. 8-19.

CNR (1979), Wideband HF channel measurement studies, CNR Final Report to Naval Research Laboratory, Washington, DC, under Contract No. W00173-77-C-0249 (CNR, Inc., Needham Heights, MA).

Cook, C.E., F.W. Ellersick, L.B. Milstein, and D.L. Schilling (Eds.) (1982), Special Issue on Spread-Spectrum Communications, IEEE Trans. Commun. COM-30, pp. 817-1070.

Cook, C.E., and H.S. Marsh (1983), An introduction to spread spectrum, IEEE Commun. Mag. 21, March, pp. 8-16.

Coon, R.M., E.C. Bolton, and W.E. Bensema (1969), A simulator for HF atmospheric radio noise, Technical Report ERL 128 - ITS 90 (ESSA/ITS, Boulder, CO).

Crozier, S., K. Tiedemann, R. Lyons, and J. Lodge (1982), An adaptive maximum likelihood sequence estimation technique for wideband HF communications, MILCOM'82 Record, pp. 29.3.1-29.3.9 (Boston, MA).

Daly, R.F. (1964), On modeling the time-varying frequency-selective radio channel, SRI Technical Report 2-Part II for the Radio Propagation Agency (U.S. Army, Ft. Monmouth, NJ).

David, F., A.G. Franco, H. Sherman, and L.B. Shucavague (1969), Correlation measurements on an HF transmission link, IEEE Trans. Commun. Technol. COM-17, pp. 245-256.

Davies, K. (1965), Ionospheric Radio Propagation, NBS Monograph No. 80, (NTIS Order No. PB 257-342/6ST).

Dentino, M., J. McCool, and B. Widrow (1978), Adaptive filtering in the frequency domain, Proc. IEEE 66, pp. 1658-1659.

Dhar, S., and B.D. Perry (1982), Equalized megahertz-bandwidth HF channels for spread spectrum communications, MILCOM'82 Record, pp. 29.5.1-29.5.5 (Boston, MA). [Also available as Report M82-46, MITRE Corp., Bedford, MA.]

Di Toro, M.J. (1968), Communication in time-frequency spread media using adaptive equalization, Proc. IEEE 56, pp. 1653-1679.

Dixon, R.C. (1984), Spread Spectrum Systems, 2nd Edition (John Wiley & Sons, New York, NY).

Ehrman, L. (1984), Wideband simulator for testing HF radios and modems, EASCON'84 Record.

Ehrman, L., L.B. Bates, J.F. Eschle, and J.M.Kates (1982), Real-time software simulation of the HF radio channel, IEEE Trans. Commun. COM-30, pp. 1809-1817. [Also available as a Signatron Report to the U.S. Air Force, RADC, Signatron, Inc., Lexington, MA.]

Evans, J.V. (1975), High power radar studies of the ionosphere, Proc. IEEE 63, pp. 1636-1650.

Folkestad, K. (Ed.) (1968), Ionospheric Radio Communications (Plenum Press, New York, NY).

Forney, G.D. (1972), Maximum-likelihood sequence estimation of digital sequences in the presence of intersymbol interference, IEEE Trans. Inform. Theory IT-18, pp. 363-378.

Geraniotis, E.A., and M.B. Pursley (1985), Performance of coherent direct-sequence spread-spectrum communications over specular multipath fading channels, IEEE Trans. Commun. COM-33, pp. 502-508.

Geraniotis, E.A., and M.B. Pursley (1986), Performance of noncoherent direct-sequence spread-spectrum communications over specular multipath fading channels, IEEE Trans. Commun. COM-34, pp. 219-226.

Gerhardt, L.A., and R.C. Dixon, (Eds.) (1977), Special Issue on Spread Spectrum Communications, IEEE Trans. Commun. COM-25, pp. 745-869.

Gersho, A. (1969), Adaptive equalization of highly dispersive channels for data transmission, Bell Sys. Tech. J. 48, pp. 55-70.

Goldberg, B. (1966), 300 kHz--30 MHz MF/HF, IEEE Trans. Commun. Technol. COM-14, pp. 767-784.

Haines, D.M., and B. Weijers (1985), Embedded HF channel probes/sounders, MILCOM'85 Record, pp. 12.1.1-12.1.7, Boston, MA.

Haydon, G.W., D.L. Lucas, and R.A. Hanson (1969), Technical considerations in the selection of optimum frequencies for high frequency sky-wave communication services, ESSA Technical Report ERL 113-ITS 81 (ESSA/ITS, Boulder, CO).

Haydon, G.W., M. Leftin, and R. Rosich (1976), Predicting the performance of high frequency sky-wave telecommunication systems [The use of the HFMUFES 4 program], OT Report 76-102 (NTIS Order No. PB 258-556/AS).

Hoff, L.E., and A.R. King (1981), Sky-wave communication techniques: Decision feedback equalization for serially modulated spread-spectrum signals in the HF band yields improved reliability, NOSC Technical Report TR 709 (Naval Ocean Systems Center, San Diego, CA).

Hoffmeyer, J.A., and W.J. Hartman (1984), LOS Microwave channel simulation--a survey of models, realizations and new concepts, 34th Symposium of the Electromagnetic Wave Propagation Panel, NATO Advisory Group for Aerospace Research and Development, Athens, Greece, June.

Holmes, J.K. (1982), Coherent Spread Spectrum Systems (John Wiley & Sons, New York, NY).

Jull, E.V. (1984), URSI Radio Science in Canada 1981-1983, URSI XXI General Assembly (Florence, Italy).

Kailath, T. (1961), Communication via randomly varying channels, Doctor of Science Thesis (MIT, Cambridge, MA).

Kashian, H.C., D.C. Rogers, and J.R. Walker (1982), Propagation measurements over geographically diverse paths, MILCOM'82 Record, pp. 29.1.1-29.1.6 (Boston, MA).

Kennedy, R.S. (1969), Fading Dispersive Communication Channels (Wiley-Interscience, New York, NY).

Koch, J.W., W.M. Beery, and H.E. Petrie (1960), Experimental studies of fading and phase characteristics of high-frequency CW signals propagated through auroral regions, NBS Report 6701 (National Bureau of Standards, Boulder, CO).

Low, J., and S.M. Waldstein (1982), A direct sequence spread-spectrum modem for wideband HF channels, MILCOM'82 Record, pp. 29.6.1-29.6.6 (Boston, MA). [Also available as Report M82-38, MITRE Corp., Bedford, MA.]

Lucas, D.L., and G.W. Haydon (1966), Predicting statistical performance indexes for high frequency ionospheric telecommunications systems, ESSA Technical Report IER 1-ITSA 1 (NTIS Order No. AD 644-827).

Lucky, R.W. (1965), Automatic equalization for digital communication, Bell Sys. Tech. J. 44, pp. 547-588.

Mahmood, N. (1983), Spread spectrum communication system for civil use, Wireless World, March, pp. 76-80.

Malaga, A. (1985), A characterization and prediction of wideband HF sky-wave propagation, MILCOM'85 Record, pp. 12.5.1-12.5.8 (Boston, MA).

Middleton, D. (1979a), Procedures for determining the parameters of the first-order canonical models of Class A and Class B electromagnetic interference [10], IEEE Trans. Electromag. Comp. EMC-21, pp. 190-208.

Middleton, D. (1979b), Canonical non-Gaussian noise models: Their implications for measurement and for prediction of receiver performance, IEEE Trans. Electromag. Comp. EMC-21, pp. 209-220.

Milsom, J.D., and T. Slator (1982), Consideration of factors influencing the use of spread spectrum on HF sky-wave paths, Second Conf. on HF Commun. Systems and Techniques (London, UK). [Also available as IEE Publication No. 206, pp. 71-74.]

Milstein, L.M., R.L. Pickholz, and D.L. Schilling (1980), Optimization of the processing gain of an FSK-FH system, IEEE Trans. Commun. COM-28, pp. 1062-1079.

Monsen, P. (1974), Adaptive equalization of the slow fading channel, IEEE Trans. Commun. COM-22, pp. 1064-1075.

Monsen P. (1977), Theoretical and measured performance of a DFE modem on a fading multipath channel, IEEE Trans. Commun. COM-25, pp. 1144-1153.

Monsen, P. (1980), Fading channel communications, IEEE Commun. Mag. 18, January, pp. 16-25.

Mueller, K.H., and D.A. Spaulding (1975), Cyclic equalization--a new rapidly converging equalization technique for synchronous data communication, Bell Sys. Tech. J. 54, pp. 370-406.

NBS (1948), Ionospheric Radio Propagation, National Bureau of Standards Circular 462 (U.S. Government Printing Office, Washington, DC).

Nupen, W. (1960), Bibliography on ionospheric propagation of radio waves (1923-1960), NBS Technical Note 84, National Bureau of Standards (Boulder, CO).

Perl, J.M., and D. Kagan (1986), Real-time HF channel parameter estimation, IEEE Trans. Commun. COM-34, pp. 54-58.

Perry, B.D. (1983a), A new wideband HF technique for MHz-bandwidth spread-spectrum radio communications, IEEE Commun. Mag. 21, September, pp. 28-36.

Perry, B.D. (1983b), Preliminary measurement of reciprocity effects on Megahertz-bandwidth equalized HF sky-wave paths, MITRE Report M83-7 (MITRE Corp., Bedford, MA).

Price, R., and P.E. Green, Jr. (1958), Communication technique for multipath channels, Proc. IRE 46, pp. 555-570.

Price, R., and P.E. Green, Jr. (1960), Signal processing in radar astronomy--Communication via fluctuating multipath media, Lincoln Lab. Technical Report 234 (Lincoln Laboratory, Lexington, MA).

Pursley, M.B. (1981), Effects of specular multipath fading on spread-spectrum communications, in New Concepts in Multi-User Communications, NATO Advanced Study Institute-Series E, J.K. Skwirzynski (Ed.) (Alphen & Noordhoff, Sijthoff aan den Rijn, The Netherlands).

Qureshi, S, (1982), Adaptive equalization, IEEE Commun. Mag. 20, March, pp. 9-16.

Rappaport, S.S., and D.M. Grieco (1984), Spread-spectrum signal acquisition: Methods and technology, IEEE Commun. Mag. 22, June, pp. 6-21.

Raut, R.N. (1980), Spread-spectrum signal communication over a fading channel: A simulation study, Journal of the Institution of Electronics and Telecommunication Engineers (New Delhi, India) 26, pp. 57-62.

RCA (1985), HF frequency hopping FACS: Frequency agile communication system, RCA Sales Brochure (RCA, Camden, NJ).

Reinisch, B.W., K. Bibl, M. Ahmed, H. Soicher, F. Gorman, and J.C. Jodogne (1984), Multipath and Doppler observations during trans-Atlantic digital HF propagation experiments, Paper No. 12, AGARD/EPP Symposium on Propagation Influences on Digital Transmission System--Problems and Solutions (Athens, Greece).

Salaman, R.K. (1962), A new ionospheric multipath reduction factor (MRF), IRE Trans. Commun. Systems CS-10, pp. 221-222.

Salous, S. (1985), Measurement of the coherent bandwidth of HF sky-wave radio links, Third Conf. on HF Commun. Systems and Techniques (London, UK). [Also available as IEE Publication No.245, pp. 62-66]

Shaver, H.N., B.C. Tupper, and J.B. Lomax (1967), Evaluation of a Gaussian HF model, IEEE Trans. Commun. Technol. COM-15, pp. 79-85.

Siess, E.W., and C.L. Weber (1986), Acquisition of direct sequence signals with modulation and jamming, IEEE J. Sel. Areas Commun. SAC-3, pp. 254-272.

Sifford, B.M., H.N. Shaver, R.F. Daly, and K.D. Felperin (1965), HF time- and frequency-dispersion effects: Experimental validation of an FSK error-rate model, SRI Technical Report 4, Stanford Research Institute (Menlo Park, CA).

Signatron (1980), High frequency channel simulator, Technical Order A250-19, Submitted to the Dept. of the Air Force, RADC/ DCLF (Signatron, Inc., Lexington, MA).

Simon, M.K., J.K. Omura, R.A. Scholtz, and B.K. Levitt (1985), Spread Spectrum Communications, Volumes I, II, and III (Computer Science Press, Rockville, MD).

Skaug, R. (1981), Experiments with spread spectrum modulation on radiowaves reflected from the ionosphere, Arch. Electron und Uebertragungstechn 35 (Germany), pp. 151-155.

Skaug, R. (1982), An experiment with spread spectrum modulation on an HF channel, Second Conf. on HF Commun. Systems and Techniques (London, UK). [Also available as IEE Publication No. 206, pp. 76-80.]

Skaug, R. (1984), Experiment with spread spectrum modulation on an HF channel, IEE Proc. 131 (Part F), pp. 87-91.

Skaug, R. (1985), Spread Spectrum in Communication (Peter Peregrinus Ltd, London , UK).

Spaulding, A.D., and D. Middleton (1977), Optimum reception in an impulsive interference environment--Part I: Coherent detection, and Part II: Incoherent detection, IEEE Trans. Commun. COM-25, pp. 910-934.

Sues, L.W., and D.M. Haines (1984), HF modem on-air tests, Report RADC-TR-84-175, Rome Air Development Center (Griffiss Air Force Base, NY).

Sunde, E. (1961), Pulse transmission by AM, FM and PM in the presence of phase distortion, Bell Sys. Tech. J., Vol. XL, pp 353-423.

Taylor, D.P., and M. Shafi (1983), A simple method for estimating multipath fade model parameters from measurements on existing analog links, IEEE Trans. Commun. COM-31, pp. 1103-1109.

Teters, L.R., J.L. Lloyd, G.W. Haydon, and D.L. Lucas (1983), Estimating the performance of telecommunication systems using the ionospheric transmission channel: Ionospheric communications analysis and prediction program user's manual, NTIA Report 83-127 (NTIS Order No. PB 84-111210).

Thrower, K.R. (1978), Systems and design considerations for spread spectrum radios, IEE Conf. on Radio Receivers and Associated Systems (Southampton, UK), pp. 413-425.

Tsui, E.T., and R.Y. Ibaraki (1982), An adaptive spread spectrum receiver for multipath/scatter channels, MILCOM'82 Record, pp. 35.3.1-35.3.5 (Boston, MA).

Turin, G.L. (1980), Introduction to spread-spectrum antimultipath techniques and their application to urban digital radio, Proc. IEEE 68, pp. 328-353.

Wagner, L.S., and J.A. Goldstein (1982), Wideband HF channel prober timing and control modules, NRL Memorandum Report 4933 (Naval Research Laboratory, Washington, DC).

Wagner, L.S., and J.A. Goldstein (1985), High-resolution probing of the HF ionospheric sky-wave channel: F2 layer results, Radio Sci. 20, pp. 287-302.

Wagner, L.S., J.A. Goldstein, and E.A. Chapman (1983), Wideband HF channel prober: System description, NRL Report 8622 (Naval Research Laboratory, Washington, DC).

Walzman, T., and M. Schwartz (1973), Automatic equalization using the discrete frequency domain, IEEE Trans. Inform. Theory IT-19, pp. 59-68.

Watterson, C.C. (1979), Methods of improving the performance of HF digital radio systems, NTIA Report 79-29 (NTIS Order No. PB 80-128606/AS).

Watterson, C.C. (1981), HF channel-simulator measurements on the KY-879/P FSK burst-communication modem-Set 1, NTIA Contractor Report 81-13 (NTIS Order No. PB 82-118944).

Watterson, C.C., J.R. Juroshek, and W.D. Bensema (1969), Experimental verification of an ionospheric channel model, ESSA Tech. Report ERL112-ITS80 (ESSA/ITS, Boulder, CO).

Watterson, C.C., J.R. Juroshek, and W.D. Bensema (1970), Experimental confirmation of an HF channel model, IEEE Trans. Commun. COM-18, pp. 792-803.

Watterson, C.C., and C.M. Minister (1975), HF channel-simulator measurements and performance analyses on the USC-10, ACQ-6, and MX-190 PSK modems, OT Report 75-56 (NTIS Order No. COM 75-11206).

Watts, J.M., and K. Davies (1960), Rapid frequency analysis of fading radio signals, J. of Geophys. Res. 65, pp. 2295-2301.

Wright, J.W., and R.W. Knecht (1957), The IGY 1957-1958 atlas of ionograms, Special CRPL Publication, National Bureau of Standards (Boulder, CO).

FORM **NTIA-29**
(4-80)

U.S. DEPARTMENT OF COMMERCE
NAT'L. TELECOMMUNICATIONS AND INFORMATION ADMINISTRATION

BIBLIOGRAPHIC DATA SHEET

	1. PUBLICATION NO.	2. Gov't Accession No.	3. Recipient's Accession No.
	NTIA Report 87-221		

4. TITLE AND SUBTITLE

Wideband HF Channel Modeling and Simulation

5. Publication Date
July 1987

6. Performing Organization Code

7. AUTHOR(S)
James A. Hoffmeyer and Martin Nesenbergs

9. Project/Task/Work Unit No.
7910 5422

8. PERFORMING ORGANIZATION NAME AND ADDRESS
National Telecommunications and Information Admin.
Institute for Telecommunication Sciences
325 Broadway
Boulder, CO 80303

10. Contract/Grant No.

11. Sponsoring Organization Name and Address
U.S. Army Joint Test Element
Joint Tactical Command, Control, and
Communications Agency
Fort Huachuca, AZ 85613-7020

12. Type of Report and Period Covered

13.

14. SUPPLEMENTARY NOTES

15. ABSTRACT *(A 200-word or less factual summary of most significant information. If document includes a significant bibliography or literature survey, mention it here.)*

Laboratory testing of proposed and new wideband (e.g., spread spectrum) high frequency (HF) systems is currently not possible because wideband HF channel simulators do not exist. Moreover, there are no validated HF channel models for bandwidth on the order of a megahertz on which to base simulator designs with confidence. Enhanced measurement programs over appropriate radio paths are needed to verify the main features of wideband channel models or to propose improvements in the existing narrowband models.

continued on reverse

16. Key Words *(Alphabetical order, separated by semicolons)*

Key words: channel simulation; HF channel models; HF propagation; spread spectrum; wideband communications

17. AVAILABILITY STATEMENT

☒ UNLIMITED.

☐ FOR OFFICIAL DISTRIBUTION.

18. Security Class. *(This report)*
Unclassified

20. Number of pages
100

19. Security Class. *(This page)*
Unclassified

21. Price:

☆ U.S. Government Printing Office: 1980—678-495/529

15. ABSTRACT (con.)

This report starts with an elementary review of ionospheric propagation. It summarizes the recent work in spread spectrum technology targeted for the HF radio band. Thereafter follows a short section devoted to additive distortions, namely noise and interference, also in the HF band. The report next presents an assessment of past narrowband HF models: their background, old validation tests, and--to be quite specific--the NTIA/ITS development of the Watterson simulator. That laboratory tool, judged best by many, works in real time and offers accurate representations of HF channel bandwidth up to 10 or 12 kHz.

In the present study, an extension to wideband models is attempted. Unfortunately, it suffers from an apparently serious shortage of measured data for the time-varying channel transfer function. A possible wideband model is hypothesized, conjectures are made, and questions are raised. One is left faced with a requirement for an experimental program to ascertain the wideband (1 MHz or more) characteristics of multipath fading for digital radio transmissions in the (2- to 30-MHz) band and over radio propagation paths of interest. Real data on the characteristics of the time-varying channel transfer function would be invaluable for the ongoing simulator work at several research organizations.